Kaposi's Sarcoma-Associated Herpesvirus Induces Sustained NF-κB Activation during De Novo Infection of Primary Human Dermal Microvascular Endothelial Cells That Is Essential for Viral Gene Expression[∇]

Sathish Sadagopan, Neelam Sharma-Walia, Mohanan Valiya Veettil, Hari Raghu, Ramu Sivakumar, Virginie Bottero, and Bala Chandran*

Department of Microbiology and Immunology, H. M. Bligh Cancer Research Laboratories, Chicago Medical School, Rosalind Franklin University of Medicine and Science, North Chicago, Illinois

In vitro Kaposi's sarcoma-associated herpesvirus (KSHV) infection of primary human dermal microvascular endothelial (HMVEC-d) cells and human foreskin fibroblast (HFF) cells is characterized by the induction of preexisting host signal cascades, sustained expression of latency-associated genes, transient expression of a limited number of lytic genes, and induction of several cytokines, growth factors, and angiogenic factors. Since NF-κB is a key molecule involved in the regulation of several of these factors, here, we examined NF-κB induction during de novo infection of HMVEC-d and HFF cells. Activation of NF-κB was observed as early as 5 to 15 min postinfection by KSHV, and translocation of p65–NF-κB into nuclei was detected by immunofluorescence assay, electrophoretic mobility shift assay, and p65 enzyme-linked immunosorbent assay. IκB phosphorylation inhibitor (Bay11-7082) reduced this activation significantly. A sustained moderate level of NF-κB induction was seen during the observed 72 h of in vitro KSHV latency. In contrast, high levels of ERK1/2 activation at earlier time points and a moderate level of activation at later times were observed. p38 mitogen-activated protein kinase was activated only at later time points, and AKT was activated in a cyclic manner. Studies with UV-inactivated KSHV suggested a role for virus entry stages in NF-κB induction and a requirement for KSHV viral gene expression in sustained induction. Inhibition of NF-κB did not affect target cell entry by KSHV but significantly reduced the expression of viral latent open reading frame 73 and lytic genes. KSHV infection induced the activation of several host transcription factors, including AP-1 family members, as well as several cytokines, growth factors, and angiogenic factors, which were significantly affected by NF-κB inhibition. These results suggest that during de novo infection, KSHV induces sustained levels of NF-κB to regulate viral and host cell genes and thus possibly regulates the establishment of latent infection.

Kaposi's sarcoma (KS) is a chronic inflammation-associated malignancy characterized by spindle-shaped endothelial cells, inflammatory cells, growth factors, and cytokines. KS is an AIDS-defining vascular tumor, and in the absence of human immunodeficiency virus type 1 infection, KS occurs in three distinct epidemiologic forms, the classic KS, endemic-aggressive KS, and transplantation-associated KS. Chang et al. (12) reported the identification of a novel herpesvirus DNA sequence, KS-associated herpesvirus (KSHV) (also called human herpesvirus 8), in all four types of KS lesions, suggesting a potential common etiological factor for KS. KSHV is also etiologically associated with two lymphoproliferative disorders, namely, body cavity-based B-cell lymphoma (BCBL) and primary effusion lymphoma (PEL) (11), and some forms of multicentric Castleman's disease. BCBL cell lines, such as BCBL-1 and BC-3, carry KSHV in a latent form, and a lytic cycle can be induced by chemical agents (56).

KSHV DNA and transcripts have been detected in B cells from the peripheral blood, B cells in BCBL and multicentric Castleman's disease, flat endothelial cells lining the vascular spaces of KS lesions, typical KS spindle cells, CD45+/CD68+ monocytes in KS lesions, keratinocytes, and epithelial cells (15, 17, 43). KSHV DNA is present in a latent form in the vascular endothelial and spindle cells of KS tissues, and expression of latency-associated LANA-1 (open reading frame [ORF] 73), v-cyclin D (ORF 72), v-FLIP (K13), and kaposin (K12) genes has been demonstrated in these cells (15, 17, 56, 63, 78). Lytic infection has also been detected in KS lesions, with <1% of infiltrating inflammatory monocytic cells positive for lytic cycle proteins (15, 17). In addition, KSHV lytic cycle K5 gene expression has been also detected in the endothelial cells and spindle cells of KS tumors (30, 65).

KSHV infects a variety of in vitro target cells, such as human B, endothelial, and epithelial cells and fibroblasts (1, 2). We have previously demonstrated that within 5 min postinfection (p.i.) of adherent target cells, KSHV induced the preexisting host cell signal pathways, such as FAK, Src, phosphatidylinositol 3-kinase (PI 3-K), Rho GTPases, PKCζ, MEK1/2, and ERK1/2 (44, 57, 58). In contrast to alpha- and betaherpesviruses, in vitro infection by KSHV does not result in a productive lytic cycle. Instead, KSHV infection of primary human dermal microvascular endothelial (HMVEC-d) cells and hu-

* Corresponding author. Mailing address: Department of Microbiology and Immunology, Chicago Medical School, Rosalind Franklin University of Medicine and Science, 3333 Green Bay Road, North Chicago, IL 60064. Phone: (847) 578-8822. Fax: (847) 578-3349. E-mail: bala.chandran@rosalindfranklin.edu.

man foreskin fibroblasts (HFF) is characterized by the sustained expression of latency-associated ORFs 73, 72, and K13. A unique aspect of this in vitro infection is our demonstration of the concurrent expression of a limited set of lytic cycle genes with antiapoptotic and immune modulation functions, including the lytic cycle switch ORF 50, or the RTA gene (30). While the expression of latent ORF 72, 73, and K13 genes continued, that of nearly all lytic genes declined (7, 30). Further examination revealed a steady quantitative increase in early lytic K5, K8, and v-IRF2 gene expression (57). KSHV-K5 gene expression persisted throughout the 5-day period of observation (30), and down regulation of major histocompatibility complex classes IA and -C, ICAM-1, CD31/PECAM, and B7-2 molecules could be detected for up to 5 days in the infected HMVEC-d cells (14, 20, 70). Similar to our observation, very early ORF 50 expression and subsequent decline were also seen during primary KSHV infection of human 293 cells (36). Bechtel et al. (7) showed that 10 of the 29 RNA transcripts detected in our system coding ORFs, such as K8.1, K12, ORF 58/59, and ORF 54, were present in the purified virion particles. However, other transcripts detected by us were absent, suggesting de novo transcription of the remaining lytic genes during the initial hours of infection. The characteristic expression of limited lytic cycle genes could be a "strategy" that allows KSHV to evade the immune system and to provide necessary factors and time to establish and/or maintain latency during the initial phases of infection. Establishment of latent infection by KSHV thus provides a good in vitro model for studying viral and host factors involved in the establishment and maintenance of latent infection. How KSHV achieves selective activation of RTA-responsive genes without initiating the full lytic cascade is a challenge to the understanding of KSHV latency. The newly synthesized ORF 73 protein can potentially influence the functions of ORF 50, since LANA-1 has been shown to counter the transactivation of certain lytic promoters by RTA. However, this may not be fully effective at early times during primary infection in the presence of abundant RTA (30). Our hypothesis is that KSHV-induced signal cascades and host cell reprogramming induced during primary infection may play important roles in the establishment of latent infection and in suppression of the lytic cycle.

As an initial step toward understanding how KSHV establishes in vitro latent infection, we have previously examined the modulation of host cell gene expression at 2 and 4 h p.i. of primary HMVEC-d and HFF cells using oligonucleotide arrays (46). We observed the reprogramming of host transcription regulating apoptosis, cell cycle regulation, signaling, inflammatory response, and angiogenesis (46). Notable among these was the strong induction of several proinflammatory cytokines and growth factors (46). Since several of these factors could be induced by NF-κB, here, we examined the induction of NF-κB early during target cell infection and its role in KSHV infection.

NF-κB belongs to a highly conserved family of transcription factors with an N-terminal Rel homology domain and a C-terminal transactivation domain that includes c-Rel, p50 (NF-κB_1), p52 (NF-κB_2), p65 (RelA), and RelB (5, 6, 21). Each of these polypeptides can form homodimers or dimerize with other Rel family members, and the prototype NF-κB is composed of p50 and p65. The function of NF-κB is regulated by a series of inhibitory molecules named IκBs. IκB molecules sequester NF-κB in the cytoplasm, thus rendering it inactive. Posttranslational modifications of IκBα, induced by various stimuli or viral infections that activate different signal transduction pathways, result in the activation of IκBα and subsequent proteolytic degradation. This causes the release of NF-κB, which translocates to the nucleus and transcribes NF-κB-dependent target genes. In lymphocytes, the IκB proteins are unstable, and high levels of NF-κB are constitutively present in the nucleus (42). In B-lymphoma cells latently infected with human gammaherpesviruses, like Epstein-Barr virus and KSHV, NF-κB activity is further elevated by the expression of latent viral gene products that activate the NF-κB signaling pathway (13, 19, 32). In Epstein-Barr virus and KSHV infections, the latency-associated proteins, like LMP1 and vFLIP, respectively, have been shown to be responsible for the sustained activation of NF-κB (69, 76). Blocking NF-κB is known to disturb latency and down regulate NF-κB-inducible cytokines, resulting in apoptosis (28, 64). However, the role played by NF-κB during primary infection of endothelial cells has not been studied.

In this study, we examined the induction of NF-κB during KSHV de novo infection of primary HMVEC-d cells and HFF and present a comprehensive view of NF-κB and the other factors induced during early and late stages of infection. We demonstrate that KSHV binding to target cells resulted in early induction of NF-κB, which was maintained at a sustained moderate level throughout the 72-h period of observation, and activated NF-κB via the AP-1 family of transcription factors playing a role in the regulation of viral and host genes, such as those encoding cytokines and growth factors.

MATERIALS AND METHODS

Cells. HFF (Clonetics, Walkersville, MD) were grown in Dulbecco's modified Eagle's medium (Gibco BRL, Grand Island, NY) supplemented with 10% heat-inactivated fetal bovine serum (HyClone, Logan, UT), 2 mM L-glutamine, and antibiotics. HMVEC-d cells (CC-2543; Clonetics) were maintained in endothelial basal medium 2 (EBM-2) in the presence of necessary growth factors (Clonetics). The cells were maintained in 5% CO_2 at 37°C. KSHV carrying BCBL-1 cells were cultured in RPMI 1640 (Gibco BRL, Grand Island, NY) medium with 10% heat-inactivated fetal bovine serum, L-glutamine, and antibiotics (44). Recombinant green fluorescent protein-KSHV (GFP-KSHV.152)-carrying BCBL-1 cells (71) were cultured in RPMI 1640 (Gibco BRL) medium (44).

Antibodies, substrates, and chemicals. Chemicals of the highest purity available were purchased. Rabbit antibodies detecting the phosphorylated forms of ERK1/2 (Thr 202/Tyr 204 phospho-p44/42 mitogen-activated protein kinase [MAPK]), p38 MAPK (Thr180/Tyr182 phospho-p38 MAPK), AKT, anti-mouse phospho-p65, total p65, total AKT, total p38 antibodies, and U0126 (1,4-diamino-2,3-dicyano-1,4-bis-[2-amino phenylthio] butadiene) were from Cell Signaling Technology, Beverly, MA. Total ERK2 antibody was from Santa Cruz Biotechnology Inc., Santa Cruz, CA. LY294002 [20(4-morpholinyl)-8-phenyl-1(4H)-benzopyran-4-one], Bay11-7082 [(E)-3-(4-methylphenylsulfonyl)-2-propenenitrile], heparin, and antibodies to β-tubulin and β-actin (clone AC-40) were obtained from Sigma, St. Louis, MO. Anti-rabbit and anti-mouse horseradish peroxidase- or alkaline phosphatase-linked antibodies were from Kirkegaard & Perry Laboratories, Inc., Gaithersberg, MD. Secondary antibodies for immunofluorescence were purchased from Molecular Probes-Invitrogen Corp., Carlsbad, CA.

Virus. The KSHV lytic cycle was induced in BCBL-1 cells, and virus from the supernatants was purified according to procedures described previously (44). Briefly, BCBL-1 cells were stimulated with 20 ng/ml of tetradecanoyl phorbol acetate (Sigma) for 6 days, and virus in the spent culture medium was concentrated and DNase treated. UV inactivation of virus was done to prepare replication-defective KSHV by inactivating the KSHV with UV light (365 nm) for 20

min at a 10-cm distance (UV-KSHV), followed by DNase treatment (57). DNA was extracted from live KSHV and UV-KSHV, and viral DNA copy numbers were quantified by real-time DNA PCR using primers amplifying the KSHV ORF 73 gene (30).

Cytotoxicity assay. Target cells were tested for their viability at various time points post-serum starvation and in the presence of various concentrations of Bay11-7082 at 37°C for different times (58, 73). EBM-2 and Dulbecco's modified Eagle's medium containing different concentrations of various inhibitors were incubated with HMVEC-d cells for 4 h. At different time points, supernatants were collected and assessed for cellular toxicity using an lactate dehydrogenase cytotoxicity assay kit (Promega, Madison, WI). The percent viabilities of HM-VEC-d cells after 8 h, 24 h, 36 h, and 48 h of serum starvation were 93%, 91%, 84%, and 81%, respectively. The viabilities of cells after 4 h of incubation with 2 μM, 5 μM, 10 μM, 15 μM, 20 μM, 25 μM, 30 μM, 35 μM, and 40 μM concentrations of Bay11-7082 were 87%, 79%, 78%, 65%, 56%, 51%, 38%, 37%, and 35%, respectively.

Western blotting. Target cells grown to confluence in 25-cm^2 flasks were serum starved and induced with KSHV (multiplicity of infection [MOI], 10, or 10 DNA copies/cell) at 37°C. For inhibitor studies, the cells were exposed to NF-κB inhibitor (Bay11-7082) for 1 h at 37°C prior to KSHV infection. After treatment, the cells were washed twice with phosphate-buffered saline (PBS), pH 7.4, and total protein was extracted. Total cell lysates (10 μg) were resolved on sodium dodecyl sulfate-polyacrylamide gel electrophoresis (SDS-PAGE) gels, transferred to nitrocellulose membranes, and immunoblotted with antibodies. Immunoreactive bands were developed by enhanced chemiluminescence reaction (NEN Life Sciences Products, Boston, MA) and quantified following standard protocols (58).

Immunofluorescence assay. HMVEC-d cells and HFF grown in eight-well chamber slides (75% confluence) (Nalge Nunc International, Naperville, IL) were serum starved, Bay11-7082 pretreated or left untreated, and incubated with KSHV for 20 min and 10 min, respectively. For colocalization studies, HMVEC-d cells were infected with KSHV for 2 h in serum-free EBM-2, followed by the addition of EBM-2 with serum and growth factors, and incubated for an additional 46 h. GFP-KSHV infection was done according to procedures described previously (59). At appropriate time points, the cells were washed with PBS, fixed with 3.7% paraformaldehyde for 10 min at room temperature, permeabilized for 10 min with 0.1% Triton X-100, and blocked for 45 min with 5% bovine serum albumin in PBS. The cells were incubated with a 1:500 dilution of rabbit anti-p65 antibody or anti-LANA antibody for 1 h at room temperature, followed by incubation with goat anti-rabbit antibody labeled with Alexa Fluor 488 (Molecular Probes-Invitrogen Corp.). After being washed with PBS, the cells were mounted with antifade reagent containing DAPI (4,6-diamidino-2-phenylindole) and observed under a fluorescence microscope equipped with the Nikon Metamorph digital imaging system 7.

Nuclear-extract preparation. HMVEC-d and HFF cells were left untreated or pretreated with Bay11-7082 at 37°C for 1 h and infected with KSHV (10 DNA copies/cell) for 15 min, 30 min, and 60 min. Nuclear extracts were prepared using a Nuclear Extract Kit (Active Motif Corp, Carlsbad, CA) according to the manufacturer's instructions. After protein concentrations were measured with bicinchoninic acid protein assay reagent (Pierce Biotechnology, Rockford, IL), the extracts were stored at −70°C. The purity of the nuclear extracts was assessed by immunoblotting using anti-lamin B antibodies, and cytoskeletal contamination was checked for by using anti-β-actin and anti-β-tubulin antibodies.

NF-κB DNA binding assay. Five micrograms of Bay11-7082-pretreated and untreated nuclear extracts was assayed for activated NF-κB by an enzyme-linked immunosorbent assay (ELISA)-based assay kit (Active Motif). This assay, which has been reported to be more sensitive than the gel shift assay, uses 96-well plates coated with oligonucleotides containing the NF-κB consensus sequence (5′-GG GACTTTCC-3′). Excess (40 pmol) mutant probe (5′-AGTTGAGGCCATTTC CCAGGC-3′) and wild-type (wt) probe (5′-AGTTGAGGGGACTTTCCCAG GC-3′) were added to reactions in the competition experiments. Plates were washed three times in wash buffer (PBS, 0.1% Tween 20), incubated with a horseradish peroxidase-conjugated anti-rabbit immunoglobulin G antibody for 1 h, washed three times, and incubated with 100 μl of developing solution for 2 to 5 min, followed by the addition of 100 μl stop solution according to the manufacturer's instructions. Plates were read with an ELISA plate reader at 450 nm with a reference wavelength of 655 nm.

EMSA. The κB and Oct1 consensus oligonucleotides were obtained from Santa Cruz Biotechnology, Inc. The double-stranded oligonucleotides were labeled at the 5′ end with [γ-^{32}P]ATP (Perkin-Elmer) using T4 polynucleotide kinase (Gibco BRL). Binding reaction mixtures were incubated on ice for 20 min, and reactions were performed in 20 μl reaction volumes containing 50 mmol/liter NaCl, 10 mmol/liter Tris-HCl, pH 7.5, 1 mmol/liter MgCl$_2$, 0.5 mmol/liter EDTA,

0.5 mmol/liter dithiothreitol, 9% (vol/vol) glycerol, 1 μg poly(dI-dC), 5 μg nuclear extract, and labeled probe (10,000 cpm). The resulting DNA-protein complexes were then size fractionated from the free DNA probe by electrophoresis at 200 V on a 5% native polyacrylamide gel. The gel was dried at 80°C and autoradiographed. A competition electrophoretic mobility shift assay (EMSA) was performed by adding a 100× molar excess of unlabeled double-stranded κB oligonucleotide probe. The nucleotide sequences of the annealed DNA probes used for κB consensus and Oct1 consensus were as follows: κB consensus, 5′-AGTTGAGGGGACTTTCCCAGGC-3′, and Oct1 consensus, 5′-TGTGGA ATGCAAATCACTAGAA-3′.

Measurement of KSHV internalization by real-time DNA PCR. Target cells that were left untreated or were treated with inhibitor were infected with KSHV at 10 DNA copies/cell. After 2 h of incubation, the cells were washed twice with PBS to remove the unbound virus, treated with trypsin-EDTA for 5 min at 37°C to remove the bound but noninternalized virus, and washed, and the total DNA was isolated using a DNeasy kit (QIAGEN, Valencia, CA). A total of 100 ng of DNA samples, KSHV-ORF 73 gene TaqMan probe (30), gene-specific primers, and Quantitect PCR mixture was used. The KSHV ORF 73 gene, cloned in the pGEM-T vector (Promega), was used for the external standard. Known amounts of ORF 73 plasmid were used in the amplification reactions, along with the test samples. The lower limit of ORF 73 gene detection was 10 to 100 copies, and the most accurate detection was from 100 to 10^6 copies. The cycle threshold values were used to plot the standard graph and to calculate the relative copy numbers of viral DNA in the samples.

Real-time RT-PCR. KSHV-infected cells, untreated or pretreated with Bay11-7082 prior to infection, were washed twice with 1× PBS to remove the unbound virus and lysed with RLT buffer (QIAGEN), and the monolayer was scraped to collect the lysate. Total RNA was isolated from the lysate (15 min, 30 min, 60 min, 90 min, 2 h, 8 h, and 24 h p.i.) using RNeasy kits (QIAGEN) according to the manufacturer's protocols, quantified spectrophotometrically, and stored at −80°C. The ORF 50, ORF 73, K5, K8, and v-IRF2 transcripts were detected by real-time reverse transcription (RT)-PCR using specific real-time primers and specific TaqMan probes as described previously (57). The expression levels of the viral transcripts were normalized to GAPDH (glyceraldehyde-3-phosphate dehydrogenase) gene expression.

Transcription factor activation assay. Five micrograms of each nuclear extract was used for the transcription factor activation assay. Transcription factors FosB, cFos, Fra1, Fra2, phospho-c-Jun, JunB, and JunD in the nuclear extracts were measured using the ELISA-based TransAM AP-1 Family kit (Active Motif Corp.) according to the manufacturer's instructions. In this assay, transcription factors bind to the immobilized oligonucleotide containing the consensus sequences specific for the particular transcription factor, which is then detected by a sandwich ELISA. The active form of the transcription factor contained in the nuclear extract specifically binds to this oligonucleotide mixture. The primary antibodies used to detect each of the AP-1 transcription factors recognize an epitope in the phosphorylated-c-Jun, JunB, JunD, cFos, FosB, Fra1, and Fra2 that is accessible only when these transcription factors are activated and bound to their target DNAs. The detection limit for the TransAM AP-1 Family kit is <0.5 μg nuclear extract/well. Competition assays were done by premixing nuclear extracts for 30 min at 4°C with wt and mutated consensus oligonucleotides provided in the kit before adding them to the probe immobilized on the plate.

Cytokine array. Conditioned media obtained by centrifuging serum-starved, untreated, or NF-κB inhibitor (Bay11-7082)-pretreated HMVEC-d cells infected with KSHV (50 DNA copies/cell) were used to study the cytokine profile using a human protein cytokine array kit from Ray Biotech (Norcross, GA). Uninfected HMVEC-d cells were used as a control. The cytokine detection membranes were blocked with a blocking buffer for 1 h at room temperature and then incubated with conditioned media at 4°C overnight. The membranes were washed, incubated with 1 ml of primary biotin-conjugated antibody at room temperature for 2 h, and subsequently washed, incubated with 2 ml of horseradish peroxidase-conjugated streptavidin at room temperature for 30 min, developed by using enhanced-chemiluminescence-type solution, exposed to film, and processed by autoradiography. Signal intensities were quantitated using an Alpha Inotech Image analysis system. All of the arrays were normalized to the same background levels with positive and negative substrate controls using the software Ray Bio Human Antibody Array 5.1 Analysis Tool.

RESULTS

KSHV induces the activation of NF-κB early during infection of HMVEC-d and HFF cells. In a normal resting cell, NF-κB is sequestered in the cytoplasm due to its association
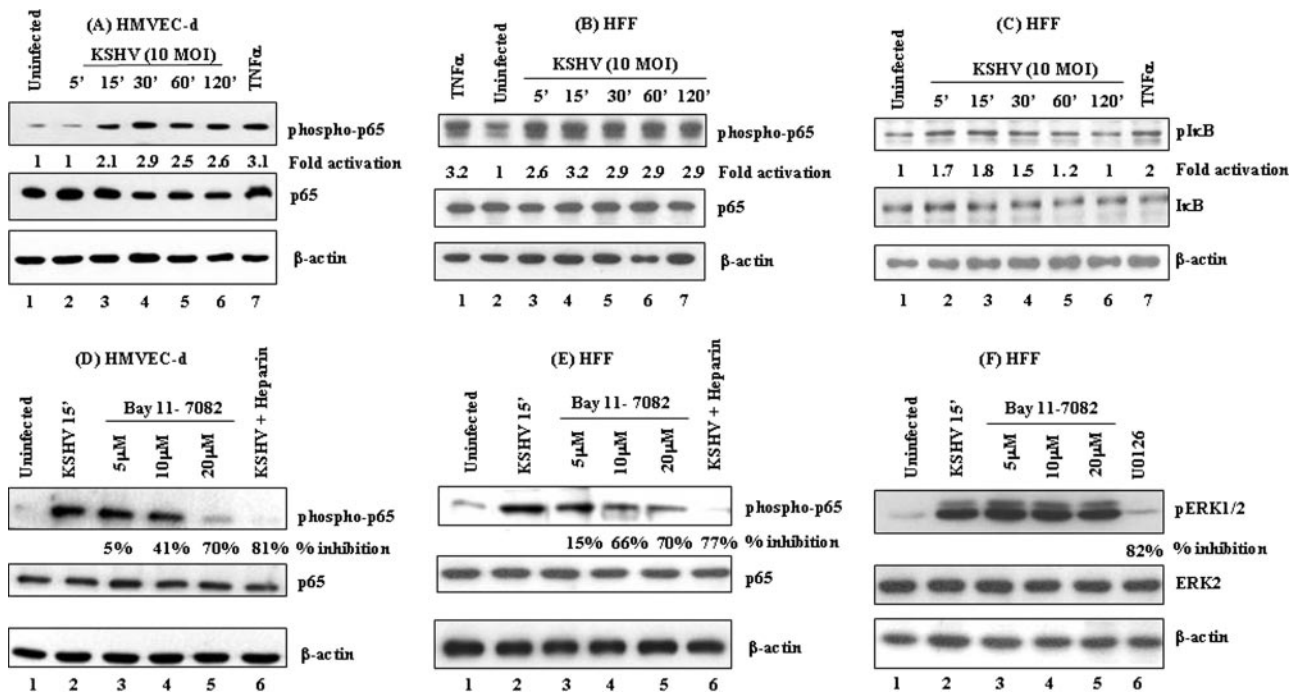
FIG. 1. (A, B, and C) Detection of activated NF-κB in KSHV-infected HMVEC-d cells and HFF. HMVEC-d cells (A) and HFF (B) grown to 80% confluence were serum starved and infected with KSHV (10 DNA copies/cell), and p65 protein phosphorylation was monitored at the indicated time points. The cells were washed and lysed with RIPA lysis buffer, and the lysates were adjusted to equal amounts of protein, resolved on SDS-10% PAGE, and transferred to nitrocellulose membranes. The membranes were immunoblotted with monoclonal antibodies against phospho-p65 protein (top), total p65 protein (middle), or β-actin (bottom). (C) HFF that were either uninfected or infected with KSHV (10 DNA copies/cell) at various time points were Western blotted using phospho-IκB (top), total IκB (middle), and β-actin (bottom) antibodies. The level of phosphorylated p65 in uninfected cells was considered to be 1 for comparison. (D, E, and F) Specificity of NF-κB induction by KSHV and inhibition by Bay11-7082. Serum-starved HMVEC-d cells (D) and HFF (E and F), untreated or pretreated with 5, 10, or 20 μM Bay11-7082 (lanes 3, 4, and 5, respectively), were either uninfected (lane 1) or infected with 10 DNA copies/cell of KSHV for 15 min. For a control, serum-starved cells were infected for 30 min with virus preincubated with 100 μg/ml of heparin for 60 min at 37°C (lane 6). The cell lysates were reacted in Western blot reactions with anti-phospho-p65 antibodies (top). The membranes were stripped and reprobed with anti-p65 antibodies (middle) and β-actin antibodies (bottom). NF-κB induction with virus alone was considered 100%, and the data are presented as the percent inhibition of p65 phosphorylation. (F) Bay11-7082-pretreated HFF lysates were immunoblotted with phospho-ERK1/2 antibodies (top, lanes 1 to 5). ERK1/2 phosphorylation in virus-infected cells was measured in the presence of the MAPK inhibitor U0126 (top, lane 6). The blots were stripped and reprobed for total ERK2 (middle) and β-actin (bottom) levels. Each blot is representative of at least three independent experiments, and percent inhibition was calculated with respect to the phosphorylated levels of p65 in KSHV-infected cells without Bay11-7082 pretreatment.

with a family of inhibitory proteins called IκB. A variety of external stimuli, like viral infections, growth factors, and cytokines, are known to phosphorylate IκB through the IKK complex, leading to the activation of NF-κB. Treatment of HMVEC-d cells and HFF with 20 ng/ml tumor necrosis factor alpha (TNF-α), a known stimulator of the NF-κB pathway, for 20 min showed about threefold increase in the phosphorylation levels of p65 and IκBα (Fig. 1A and C, lane 7; Fig. 1B, lane 1).

When target cells were infected with KSHV (10 DNA copies/cell), we observed rapid NF-κB activation, as detected by NF-κB–p65 phosphorylation as early as 15 min p.i. of HMVEC-d cells (Fig. 1A, top, lanes 1 to 6) or at 5 min p.i. of HFF (Fig. 1B, top, lanes 2 to 7). The NF-κB activation observed in both cell types was sustained until 120 min after the start of our observation. When phospho-IκB antibodies were used to determine whether p65 activation was due to IκB phosphorylation, we observed phosphorylation of IκBα in infected HFF cells as early as 5 min p.i. (Fig. 1C, top, lanes 1 to 6). NF-κB–p65 phosphorylation observed at nearly the same time points suggested that KSHV infection results in IκBα phosphorylation, which in turn could be responsible for p65

activation. Similar IκBα phosphorylation was seen in HMVEC-d cells (data not shown). Equal loading of total lysates between different treatments was confirmed by the detection of similar β-actin protein levels in all samples (Fig. 1A, B, and C, bottom). Infection did not affect the total p65 levels in both HMVEC-d cells (Fig. 1A, middle) and HFF (Fig. 1B, middle) or total IκB levels in HFF (Fig. 1C, middle). These results demonstrated that KSHV activates NF-κB early during infection of adherent HMVEC-d and HFF cells.

Specificity of KSHV-induced NF-κB activation in HMVEC-d and HFF cells. Bay11-7082 is an inhibitor of IκB phosphorylation and is known to inhibit NF-κB activation (8). To determine whether abrogation of IκB phosphorylation could inhibit KSHV-induced NF-κB activation, cells pretreated with various concentrations of Bay11-7082 were infected with KSHV for 15 min and then analyzed for NF-κB activation. We observed a dose-dependent inhibition of KSHV-induced p65 activation by Bay11-7082 in infected HMVEC-d cells and HFF (Fig. 1D and E, top, lanes 3 to 5).

KSHV binds to the adherent target cell surface heparan sulfate via its envelope glycoproteins gB and gpK8.1A (1, 72).
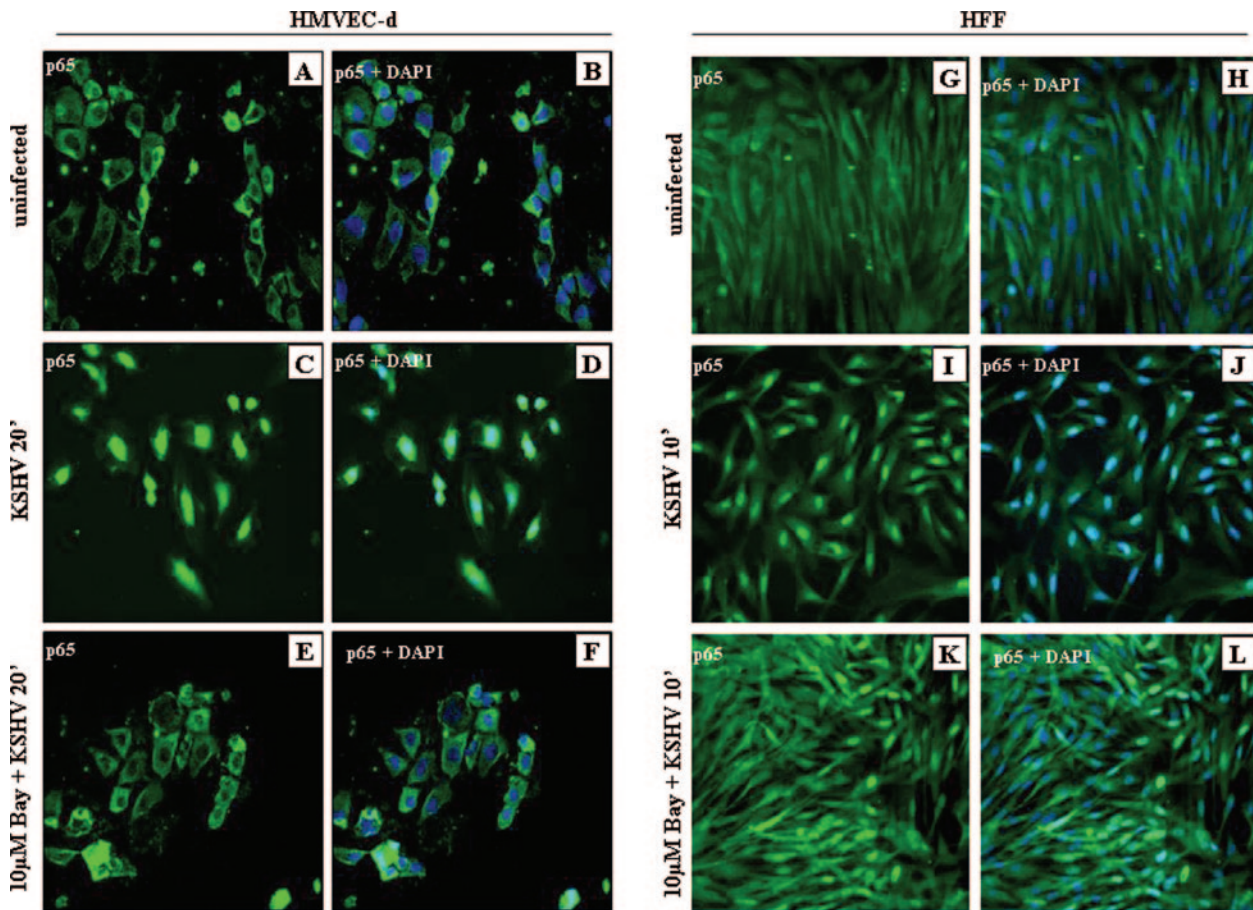
FIG. 2. Nuclear translocation of NF-κB–p65 in KSHV-infected cells. Serum-starved HMVEC-d cells and HFF grown in eight-well chamber slides were infected with KSHV (10 DNA copies/cell) for 20 min and 10 min, respectively; washed; fixed; permeabilized; and stained with anti-p65 polyclonal antibody. HMVEC-d cells and HFF were either uninfected (A, B, G, and H) or infected with KSHV (10 DNA copies/cell) (C, D, I, and J) or incubated with 10 μM Bay11-7082, followed by infection with KSHV (E, F, K, and L), and stained for NF-κB–p65. DAPI was used as a nuclear stain and merged with p65 staining.

Blocking this interaction with heparin, an analogue of heparan sulfate, prevents KSHV binding to the target cells and infection (2, 72). To demonstrate whether NF-κB activation was due to KSHV binding and entry into the target cell and not due to contaminating materials or lipopolysaccharide, cells were infected for 30 min with KSHV preincubated with heparin, and lysates were analyzed for NF-κB–p65 phosphorylation. Heparin treatment blocked the KSHV-induced NF-κB activation by about 81% and 77% in HMVEC-d cells and HFF, respectively (Fig. 1D and E, top, lane 6), indicating that NF-κB activation was indeed due to KSHV infection.

We had previously shown that KSHV infection induces a rapid transient MEK1/2 and ERK1/2 phosphorylation in HMVEC-d cells and HFF (57). When lysates from Bay11-7082-pretreated cells were tested with phospho-ERK1/2 antibodies, Bay11-7082 pretreatment had no effect on KSHV-induced ERK1/2 phosphorylation (Fig. 1F, top, lanes 3 to 5). In contrast, pretreatment of cells with 10 μM U0126, a MEK1/2-specific inhibitor, resulted in about 82% inhibition of KSHV-induced ERK1/2 phosphorylation (Fig. 1F, top, lane 6). There was no change in the total ERK2 levels (Fig. 1F, middle, lanes 1 to 6). Equal loading was confirmed using anti-β-actin anti-

bodies (Fig. 1F, bottom, lanes 1 to 6). These results demonstrated the specificity of inhibition by Bay11-7082 pretreatment, as well as the specificity of KSHV-induced NF-κB activity.

KSHV triggers the rapid nuclear translocation of activated NF-κB–p65. Once activated in a stimulus-specific manner, NF-κB rapidly translocates into the nucleus and induces the transcription of various cellular genes (48). Since KSHV induced the NF-κB early during infection, we examined the uninfected and infected cells by immunofluorescence assay using polyclonal antibody against NF-κB–p65. Rapid nuclear translocation of p65 in >90% of KSHV-infected HMVEC-d cells (Fig. 2C and D) and HFF (Fig. 2I and J) was observed 20 min and 10 min p.i., respectively. In contrast NF-κB–p65 was predominantly localized in the cytoplasm of uninfected cells (Fig. 2A, B, G, and H). Pretreatment with Bay11-7082 significantly inhibited nuclear translocation in both HMVEC-d cells (Fig. 2E and F) and HFF (Fig. 2K and L). These results confirmed the specificity of NF-κB induction and further supported our observation that KSHV induces NF-κB early during infection of target cells.

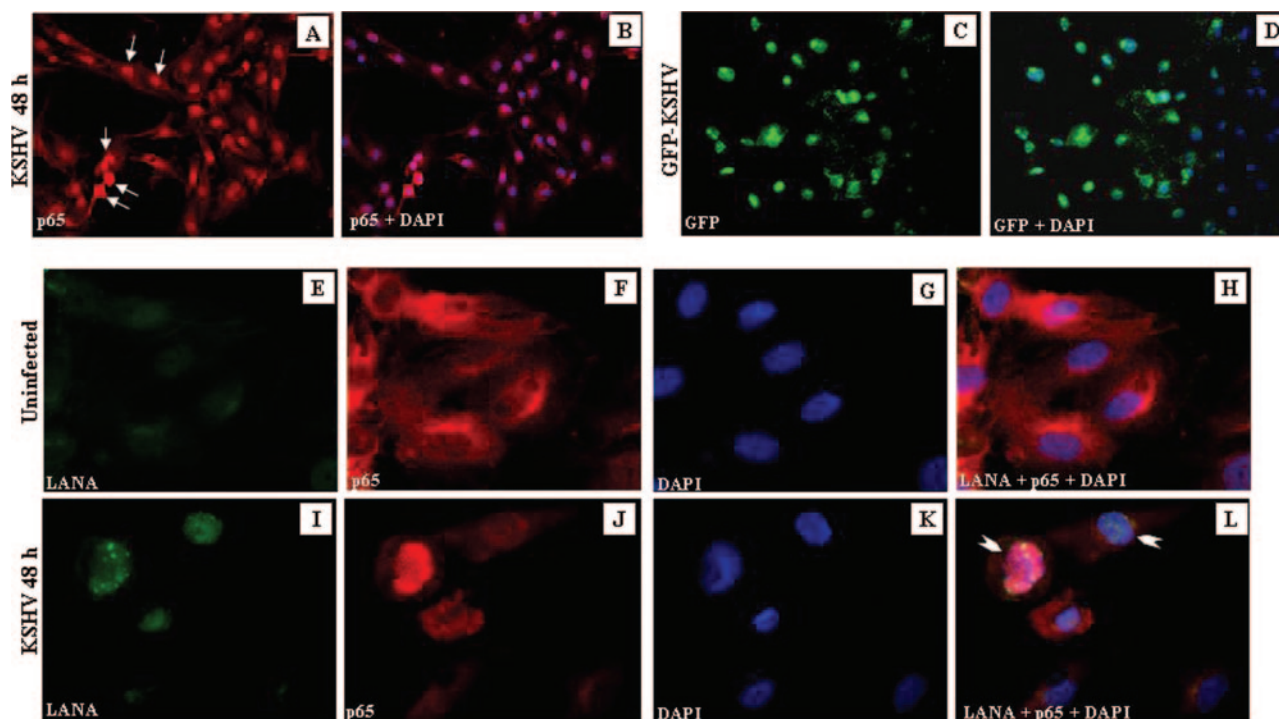When infected cells were examined at 48 h p.i., >70% of the

FIG. 3. Colocalization of NF-κB–p65 and ORF-73 (LANA-1) in KSHV-infected HMVEC-d cells. (A) Serum-starved HMVEC-d cells grown in eight-well chamber slides were infected with KSHV (10 DNA copies/cell) for 48 h, washed, fixed, permeabilized, and stained with anti-p65 polyclonal antibody. (B) Merged image of DAPI-stained nuclei with p65 staining. (C) HMVEC-d cells infected with GFP-KSHV for 48 h. (D) Merged image of DAPI-stained nuclei with GFP staining. (E to L) Colocalization of LANA-1 and p65. LANA (green in panels E and I) and p65 (red in panels F and J) in uninfected (E to H) and infected (I to L) HMVEC-d cells. (G and K) DAPI staining merged with LANA-1 and p65 (H and L). The arrows (A) indicate p65 nuclear staining, and the arrowheads (L) indicate cells positive for LANA-1 and p65 nuclear staining.

cells displayed p65 nuclear translocation (Fig. 3A and B). Infection of HMVEC-d cells with GFP-KSHV at an MOI of 10 revealed that about 60% of the cells were infected under these conditions (Fig. 3C and D). Uninfected cells were negative for ORF 73 staining and showed cytoplasmic p65 staining (Fig. 3E, F, G, and H). In contrast, cells infected with KSHV displayed characteristic punctate nuclear staining of ORF 73 protein, and greater than 50% of the cells were positive for both ORF 73 and nuclear p65 at 48 h p.i. (Fig. 3I, J, K, and L). Some of the uninfected cells also displayed p65 nuclear translocation, which could be due to the actions of cytokines and growth factors released from the HMVEC-d cells (see Fig. 9). These results suggested that NF-κB stimulation also occurs at a later time p.i., a time point when only the expression of latent KSHV genes was observed (7, 30).

KSHV infection increases the NF-κB DNA binding activity in HMVEC-d and HFF cells. After translocating into the nucleus, activated NF-κB binds to κB site sequences in the various target genes and initiates transcription. To determine whether KSHV infection induces the DNA binding activity of NF-κB, we analyzed the nuclear extracts prepared from infected untreated or Bay11-7082-pretreated cells by an ELISA-based DNA binding assay. The purity of the nuclear extracts was confirmed using anti-lamin B and anti-tubulin antibodies (reference 45 and data not shown). When infected-cell values were normalized to the uninfected-cell values, nuclear extracts from HMVEC-d cells and HFF infected for 30 min displayed enhanced NF-κB DNA binding activity (Fig. 4A). The speci-

ficity of increase in NF-κB DNA binding activity was demonstrated by inhibition using excess wt oligonucleotides, but not with excess mutant consensus site oligonucleotides (Fig. 4A). The specificity was also demonstrated by the dose-dependent decrease in NF-κB DNA binding activity in Bay11-7082-pretreated HMVEC-d cells and HFF (Fig. 4B). Time course analysis of DNA binding activity with cells pretreated with 10 μM Bay11-7082 showed inhibitions of about 45%, 58%, and 55% at 15 min, 30 min, and 60 min p.i., respectively, in HMVEC-d cells and about 72%, 65%, and 69% at 15 min, 30 min, and 60 min p.i., respectively, in HFF (Fig. 4C). These results correlated well with the Western blot data. For all further studies, 5 μM and 10 μM concentrations of Bay11-7082 were used, and only the concentration showing optimal activity is presented in the figures.

EMSA detects the increase in NF-κB DNA binding activity in infected HMVEC-d and HFF cells. To confirm the above finding, EMSA was performed to demonstrate NF-κB protein binding to the NF-κB sites. Retardation in the migration of radiolabeled NF-κB consensus site oligonucleotides was observed with infected-cell nuclear extracts (Fig. 5A and B, lanes 2 to 4) and was reduced by 10 μM Bay11-7082 pretreatment (Fig. 5A and B, lanes 5 to 7). The specificity of this reaction was demonstrated by the absence of NF-κB binding to the target DNA in the competition assays using 100 times molar excess of cold double-stranded κB oligonucleotide probe (Fig. 5A and B, lane 10), while the binding was not affected with normal probe (Fig. 5A and B, lane 11). Binding of Oct1 protein
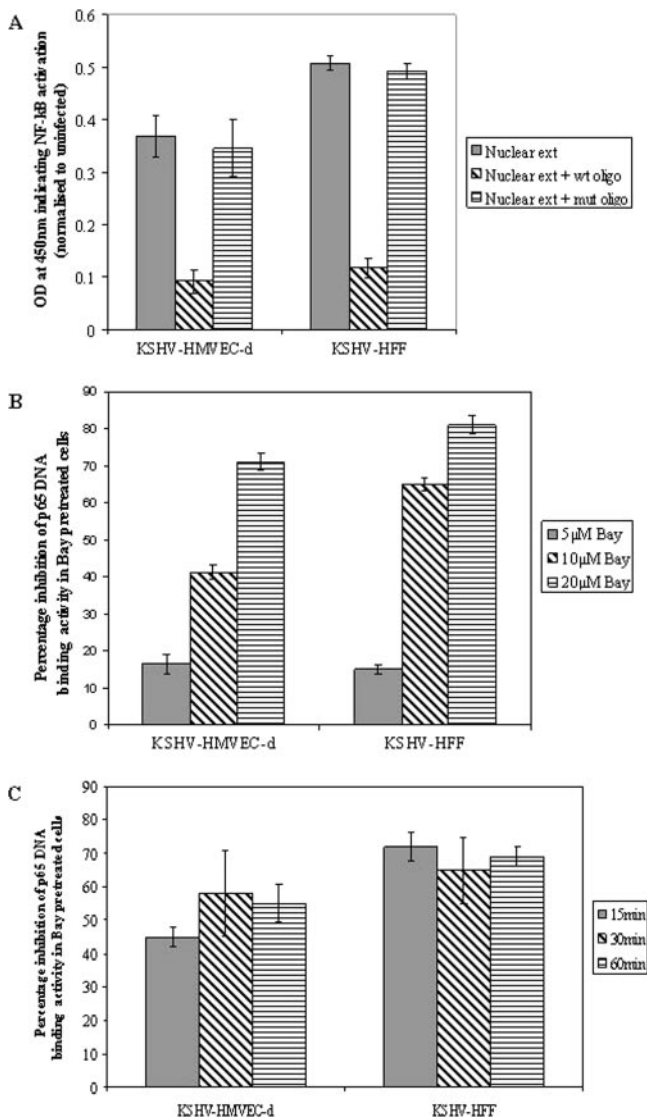
FIG. 4. Detection of KSHV-induced nuclear translocation of NF-κB–p65 by ELISA. (A) Nuclear extracts from HMVEC-d cells and HFF infected with KSHV (10 DNA copies/cell) for 30 min were prepared and assayed for NF-κB DNA binding activity by ELISA. Plates immobilized with oligonucleotides specific for the κB site were incubated with nuclear extracts (5 μg/well), followed by ELISA with anti-p65 antibody. The competition experiment was done in a similar fashion but using plates coated with excess (20 pmol) NF-κB consensus site mutant or wt oligonucleotides. The data represent the averages ± standard deviations of three experiments. (B) HMVEC-d cells and HFF untreated or pretreated with various concentrations of Bay11-7082 for 1 h were infected with KSHV (10 DNA copies/cell) for 30 min, and nuclear extracts were prepared and assayed for NF-κB DNA binding activity. The percent nuclear translocation of NF-κB–p65 inhibition by Bay11-7082 pretreatment was calculated with respect to the DNA binding activities in untreated KSHV-infected cells. (C) Histograms depicting the kinetics of percent inhibition of DNA binding activity in nuclear extracts from HMVEC-d cells and HFF pretreated with 10 μM Bay11-7082 for 1 h and then infected with KSHV (10 DNA copies/cell) for different times. The data represent the averages ± standard deviations of three experiments.

to its specific probe remained unchanged (Fig. 5A and B, bottom, lanes 1 to 11), which also demonstrated the specificity of NF-κB inhibition by Bay11-7082. These results demonstrated that KSHV infection activated NF-κB translocation to the nucleus and recognized the NF-κB-specific sites, suggesting possible transcription of NF-κB-dependent genes.

Early induction of NF-κB by KSHV indicated a role for virus binding and entry stages. To determine whether NF-κB induction requires a KSHV-induced signal cascade and/or viral gene expression, we examined the NF-κB levels in HMVEC-d cells infected with either live KSHV or UV-KSHV at an MOI of 10. Live KSHV induced NF-κB to a greater extent than UV-KSHV, with about 3.1-, 3-, and 4.2-fold increases in NF-κB activation with live KSHV (Fig. 5C) compared to 2.1-, 2.6-, and 2.5-fold with UV-KSHV (Fig. 5D) at 2 h, 8 h, and 24 h p.i., respectively, in HMVEC-d cells. Oct1 levels remained unaltered with live-KSHV and UV-KSHV infection at all time points. Although NF-κB induction with UV-KSHV was significantly higher than that of uninfected cells and was sustained, the induction was lower than the induction observed with live KSHV at all parallel time points. This suggested that early induction of NF-κB by KSHV must be mediated by virus binding and entry stages, and KSHV viral gene expression appears to be required for the continued augmented induction of NF-κB.

KSHV induces a sustained level of NF-κB induction during de novo infection of HMVEC-d and HFF cells. Early during infection of adherent target cells, KSHV induced the FAK, Src, PI 3-K, Rho-GTPase, PKC-ζ, and ERK1/2 signal pathways, which were characterized by a rapid early response, followed by decline to the resting state within 2 to 4 h of observation (31, 44, 57, 58). Since we observed NF-κB activation up to 120 min p.i. (Fig. 1) to determine the extent of NF-κB induction and to compare it to other KSHV-induced signal cascades, infected HMVEC-d cells and HFF collected at different time points p.i. were analyzed for the phosphorylated forms of NF-κB–p65, ERK1/2, AKT, and p38 MAPK. We observed a modest level of NF-κB–p65 activation in the infected HMVEC-d cells at all time points tested (Fig. 6A). Phosphorylated p65 was detected as early as 10 min p.i., and sustained activation at a >2-fold increase over that of the uninfected cells was observed until 48 h p.i. (Fig. 6A, lanes 1 to 12), as well as at 72 h p.i. (data not shown). In contrast, there was a rapid increase in ERK1/2 phosphorylation, which peaked at 30 min p.i. with about 12.5-fold activation over that of the uninfected cells and decreased by 4 h p.i., followed by a second cycle of activation, which peaked at 24 h p.i. and returned to the basal level at 48 h p.i. (Fig. 6A).

KSHV induces FAK, Src, and PI 3-K pathways, and NF-κB could be activated through the PI 3-K–AKT pathway (58). When we examined the activation of AKT, a fourfold increase in the phospho-AKT level was observed by 5 min p.i., followed by a reduction till 30 min p.i. and a second cycle of increase (2.5-fold) at 1 h, which peaked to 3.4-fold at 2 h p.i. Although the phospho-AKT level decreased between 4 and 24 h p.i., it showed a higher level of activation than the uninfected cells. A third intense eightfold activation was seen at 24 h p.i., which decreased to threefold at 48 h p.i. (Fig. 6A).

Previously, we did not observe the induction of lipopolysaccharide/stress-activated p38 MAPK during 60 min of KSHV
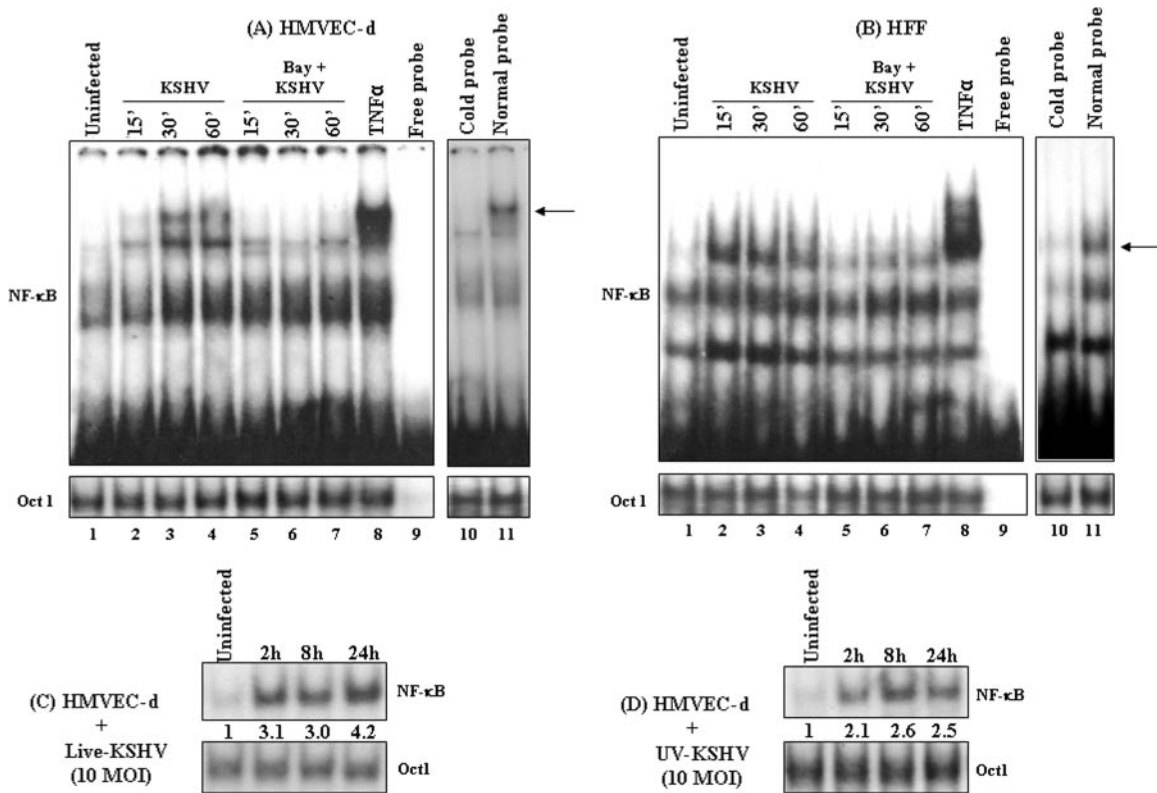
FIG. 5. EMSA detection of KSHV-induced NF-κB DNA binding activity. (A and B, top, lanes 1 to 7) HMVEC-d cells (A) and HFF (B), untreated or pretreated with 10 μM Bay11-7082 (1 h), were left uninfected or infected with KSHV (10 DNA copies/cell) for the indicated times. Nuclear extracts prepared from these cells were incubated with κB-specific probe. The specificity of DNA-protein interaction was assessed by induction with TNF-α (20 ng/ml) (lane 8), free probe (lane 9), normal probe (lane 11), or competitive EMSA using a 100× molar excess of unlabeled double-stranded oligonucleotide κB probe (cold probe; lane 10). Nuclear extracts from HMVEC-d cells infected with 10 DNA copies/cell of live KSHV (C) or UV-KSHV (D) for 2 h, 8 h, and 24 h were analyzed by EMSA. Each EMSA is representative of at least three independent experiments. (A and B, bottom, lanes 1 to 11, and C and D, bottom) Oct1 probe used as loading control and specificity control to demonstrate the binding of NF-κB to the specific probe. The arrows indicate the positions of the induced NF-κB complexes.

infection in HMVEC-d, 293, or HFF cells (44). A recent study reported that p38 MAPK activation is essential for KSHV infection in human umbilical vein endothelial cells (49). Furthermore, the KSHV latency-associated gene product kaposin B (K12-B) has been shown to enhance the release of proinflammatory cytokines by activating the p38 MAPK–MAPK-associated protein kinase 2 (MK2) pathway and blocking cytokine mRNA decay by binding to MK2 (40). Cytokines that are secreted upon KSHV infection can act in an autocrine or paracrine fashion to activate p38 MAPK. Activation of many of these cytokines is known to be controlled by NF-κB and p38 MAPK-MK2-kaposin B may play an important role in stabilizing the cytokine expression that is activated by NF-κB. Hence, we examined the kinetics of p38 MAPK activation by KSHV. In agreement with our earlier results (44), there was only minimal activation of p38 MAPK at earlier time points (Fig. 6A, lanes 2 to 7). However, an appreciable level of p38 MAPK activation was observed at 8 h p.i. with about 2.6-fold activation over that of uninfected cells, peaking at 24 h p.i. with 3.8-fold induction and returning to basal level at 48 h p.i. (Fig. 6A, lanes 8 to 12). Equal loading of samples was demonstrated by detection of similar levels of total p65, AKT, p38, ERK2, and β-actin throughout the observation period (Fig. 6A), which also clearly suggested that KSHV infection induces the

phosphorylation of these proteins without affecting the total protein synthesis levels.

KSHV-infected HFF also displayed p65, ERK1/2, AKT, and p38 MAPK activation kinetics similar to that seen in HMVEC-d cells (Fig. 6B). There was modest steady-state activation of NF-KB–p65 at all time points, which peaked at 24 h p.i. (3.4-fold activation) and reached the basal level at 72 h p.i. We observed about 8-fold ERK1/2 phosphorylation as early as 5 min p.i., which peaked at 10 min at 9.2-fold and returned to basal level between 8 and 24 h p.i. (Fig. 6B). A second cycle of moderate ERK1/2 activation was seen at 24 to 48 h p.i. (Fig. 6B, lanes 10 to 12). The induction kinetics of phospho-AKT was similar to that of HMVEC-d cells but with two cycles of activation, the first cycle starting at 5 min p.i., peaking at 2 h p.i., and returning to basal level between 4 and 12 h p.i., with a second cycle of AKT activation seen at 24 h p.i. (2.2-fold activation), which was sustained at a moderate level until 72 h p.i. (Fig. 6B, lanes 2 to 13). Similar to HMVEC-d cells, minimal activation of p38 MAPK at earlier time points was observed in HFF (Fig. 6B, lanes 2 to 5), which started to increase at 2 h p.i., reached a maximum at 12 h p.i., and returned to basal levels at 72 h p.i. (Fig. 6B, lanes 6 to 13).

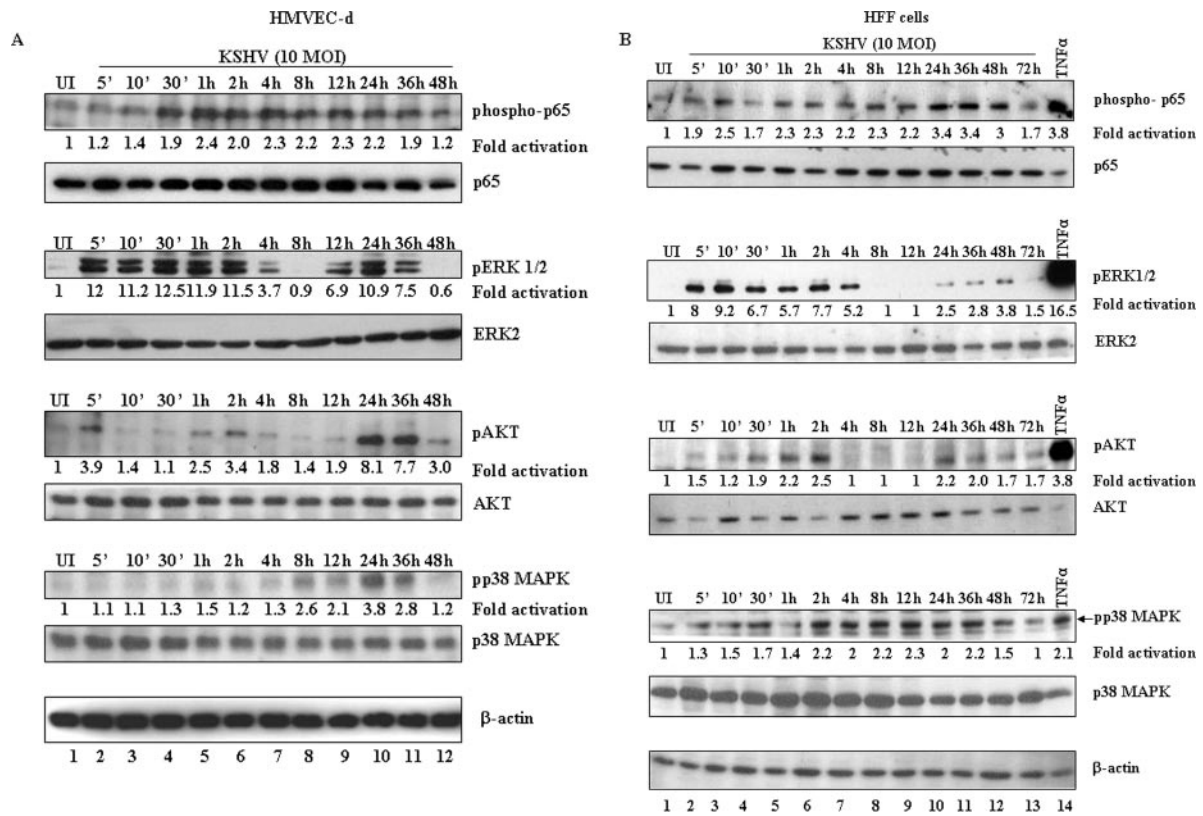Taken together, these results demonstrated that KSHV infection induces a sustained level of NF-κB during the 72-h

FIG. 6. Sustained activation of NF-κB during de novo infection of target cells by KSHV. Proteins prepared from HMVEC-d cells (A) and HFF (B) that were uninfected (UI) or infected with KSHV (10 DNA copies/cell) for 5 min, 10 min, 30 min, 1 h, 2 h, 4 h, 8 h, 12 h, 24 h, 36 h, 48 h, and 72 h were resolved by SDS-PAGE and transferred onto nitrocellulose membranes. Phosphorylated and total p65, ERK 1/2, AKT, and p38 MAPK proteins were detected with the respective antibodies. Each blot is representative of at least three independent experiments. The phosphorylation levels in the uninfected cells were considered to be 1 for comparison. For a control, cells were induced with TNF-α for 20 min.

period of observation, which is in contrast to the biphasic ERK1/2 and AKT activation and activation of p38 MAPK at later time points. These results also suggested that during primary infection of adherent target cells, KSHV must have evolved to differentially induce these signal molecules.

KSHV-induced NF-κB does not play a role in entry of virus into target cells. KSHV entry overlaps with the induction of host cell preexisting signal pathways, such as FAK, Src, PI 3-K, Rho-GTPases, PKC-ζ, and ERK1/2 (44, 57, 58). We have demonstrated the roles of FAK and PI 3-K in virus entry; the role of RhoA-GTPase in microtubule modulation, transport of capsid in the cytoplasm, and nuclear delivery; and a role for ERK1/2 in viral gene expression (31, 44, 45, 57). Target cells preincubated with the PI 3-K inhibitor LY294002 inhibited the internalization of KSHV DNA (58), whereas there was no significant reduction when cells were pretreated with the MEK/ERK inhibitor U0126 (57). To determine whether KSHV-induced NF-κB plays a role in viral infection, we examined virus DNA internalization by quantitative real-time DNA PCR for the KSHV ORF 73 gene. Treatment of cells with three different concentrations of Bay11-7082 did not have any effect on KSHV DNA entry in both HMVEC-d cells and HFF (Fig. 7A). In contrast, preincubation of cells with 50 μM LY294002 reduced internalization by about 60% and 55% in HMVEC-d cells and HFF, respectively (Fig. 7A). These results

demonstrated that KSHV-induced NF-κB does not have a significant role in viral DNA internalization.

Inhibition of NF-κB blocks the expression of KSHV latent and lytic gene expression. To analyze the potential role of NF-κB activation in KSHV gene expression, HMVEC-d cells and HFF were preincubated with different concentrations of Bay11-7082 at 37°C for 1 h and infected with KSHV for 2 h, and viral messages, collected at different time points p.i., were quantitated by real-time RT-PCR. We had previously shown that de novo KSHV infection of HMVEC-d and HFF is characterized by the sustained expression of latency-associated ORF 73 (LANA-1), ORF 72 and K13 genes and transient expression of a limited number of lytic genes, including ORF 50 (RTA), vIRF2, K8, and K5 genes (30, 57). In the present study, we also observed a steady increase in ORF 73 gene expression from as early as 15 min p.i. and peaking at 24 h p.i., while ORF 50 gene expression was 10-fold higher at initial time points, peaked at 2 h p.i., and was gradually reduced to basal levels at 24 h p.i. in HMVEC-d cells (Fig. 7B and C). As the gene expression of ORF 50 and ORF 73 was high at 2 h and 24 h, respectively, expression levels of other lytic genes, like K5, K8, and vIRF2, were studied and compared at 2 h, 8 h, and 24 h p.i. Likewise, in HFF, there was a stable increase in ORF 73 gene expression during the observed 24-h time period (Fig. 7D). In contrast, very high levels of lytic gene expression were
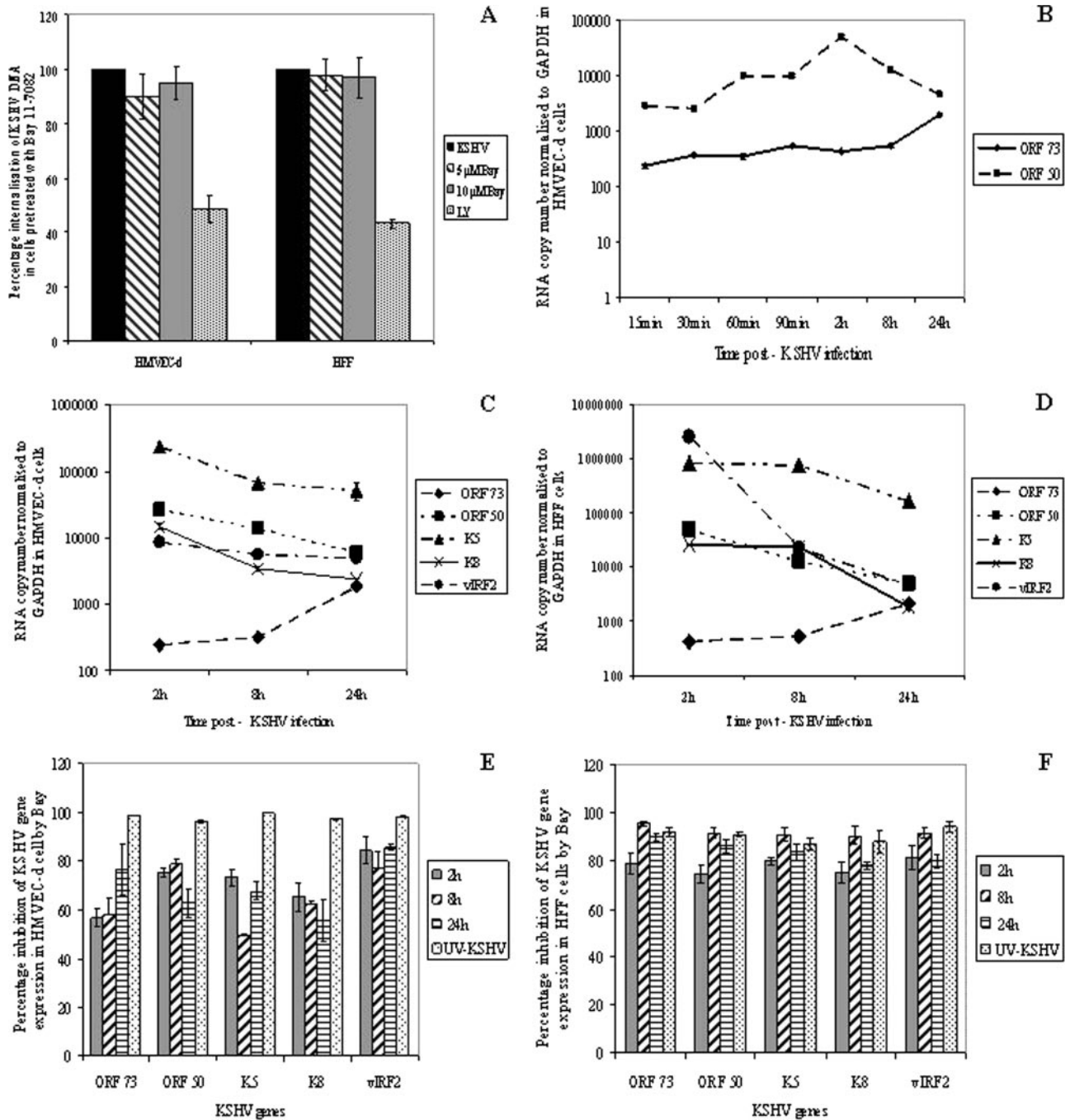
FIG. 7. Effect of Bay11-7082 on KSHV entry and KSHV ORF 73, ORF 50, K5, K8, and vIRF2 gene expression. (A) HMVEC-d cells and HFF, untreated or incubated with different concentrations of inhibitors for 1 h at 37°C, were infected with KSHV at 10 DNA copies/cell. For a control, cells were preincubated with 50 μM LY294002 (LY) for 1 h at 37°C before virus was added. After 2 h of incubation, the cells were washed twice with PBS to remove the unbound virus, treated with trypsin-EDTA for 5 min at 37°C to remove the bound but noninternalized virus, and washed, and total DNA was isolated. This was normalized, and the numbers of KSHV genome copies were estimated by real-time DNA PCR for ORF 73. The cycle threshold values were used to plot the standard graph and to calculate the relative copy numbers of viral DNA in the samples. The data are presented as the percent entry of KSHV DNA internalization obtained when the cells were incubated with virus alone. Each reaction was done in duplicate, and each bar represents the mean and standard deviation of three experiments. (B to F) Untreated HMVEC-d cells and HFF or cells pretreated with 10 μM Bay11-7082 for 1 h were infected with KSHV (10 DNA copies/cell) for 2 h, 8 h, and 24 h, and RNA was isolated and treated with DNase I for 1 h. A total of 250 ng of DNase-treated RNA was subjected to real-time RT-PCR with ORF 73, ORF 50, K5, K8, and vIRF2 gene-specific primers and TaqMan probes. Standard graphs generated using known concentrations of DNase-treated in vitro-transcribed ORF 73, ORF 50, K5, K8, and vIRF2 transcripts were used to calculate the relative copy numbers of viral transcripts and were normalized with GAPDH. Each reaction was done in duplicate, and each point represents the average ± standard deviation of three independent experiments. (B) Kinetics of ORF 73 and 50 gene expression in HMVEC-d cells. (C and D) Comparative kinetics of ORFs 73 and 50, K5, K8, and vIRF2 in HMVEC-d cells and HFF, respectively. (E and F) Histograms depicting the percent inhibition of KSHV ORF 73 and 50, K5, K8, and vIRF2 expression in the presence of Bay11-7082 in HMEVC-d cells and HFF, respectively.

seen at earlier time points, which peaked between 2 and 8 h p.i. and slowly declined thereafter in HMVEC-d cells and HFF (Fig. 7C and D). As we have previously demonstrated (57), no viral gene expression was seen when target cells were infected with UV-KSHV (Fig. 7E and F). Treatment of cells with 10 μM Bay11-7082 for 1 h reduced both latent and lytic KSHV gene expression significantly (Fig. 7E and F). The expression of the ORF 73 gene in HMVEC-d cells was reduced by about 55%, 58%, and 77% at 2 h, 8 h, and 24 h p.i., respectively (Fig. 7E). Similarly, expression of the ORF 73 gene in HFF was reduced by about 79%, 96%, and 90% at 2 h, 8 h, and 24 h p.i., respectively (Fig. 7F). About 50% to 85% reduction in the lytic genes was observed in Bay11-7082-treated HMVEC-d cells (Fig. 7E), and 75% to 95% inhibition was seen in HFF (Fig. 7F). These results demonstrated that NF-κB induced by KSHV early during target cell infection plays an important role in viral latent and lytic gene expression, thus contributing to KSHV infection and pathogenesis.

KSHV-induced NF-κB plays a major role in the activation of AP-1 family transcription factors. The roles played by NF-κB and AP-1 transcription factors independently in modulating KSHV latent and lytic gene expression in PEL cells are well documented (3, 64). However, there are no reports on the effects of NF-κB inhibition on AP-1 transcription factors during de novo KSHV infection. Our studies suggested that NF-κB activation is required for initiation of transcription of both latent and lytic genes in primary adherent target cells. To determine whether this is due to the ability of NF-κB to modulate a variety of host transcription factors, we next examined the ability of KSHV infection to induce AP-1 transcription factors, which are known to be involved in KSHV latent and lytic gene expression (57).

Nuclear extracts from uninfected and infected HMVEC-d cells were assessed in an ELISA-based assay for the ability of the AP-1 transcription factors to bind to their respective wt DNA sequences. Since we observed NF-κB activation very early during infection, nuclear extracts from HMVEC-d cells infected with KSHV for 15 min, 30 min, and 60 min were assayed for the AP-1 family of transcription factors. Infection of HMVEC-d cells with KSHV mediated a differential activation of AP-1 family transcription factors (Fig. 8). As shown in Fig. 8A, compared to uninfected cells, KSHV infection increased the activated forms of both Fos and the Jun family of transcription factors. A higher level of activation was observed for phospho-c-Jun, JunB, JunD, and cFos, while FosB, Fra1, and Fra2 transcription factors were moderately activated (Fig. 8A). Specificity experiments carried out with wt and mutated oligonucleotides demonstrated a significant reduction in the abilities of transcription factors to bind their respective target sequences by preincubation with wt oligonucleotides (data not shown).

To analyze the effect of the NF-κB inhibitor Bay11-7082 in KSHV-mediated induction of AP-1 transcription factors, HMVEC-d cells were pretreated with the drug and infected with KSHV for 15 min, 30 min, and 60 min, and the activities of various transcription factors in the nuclear extracts of infected cells were measured. Only the optimum time point values are represented in the graphs (Fig. 8B and C). In agreement with previous results (Fig. 8A), neither KSHV infection nor inhibitors of the NF-κB pathway had any effect on the
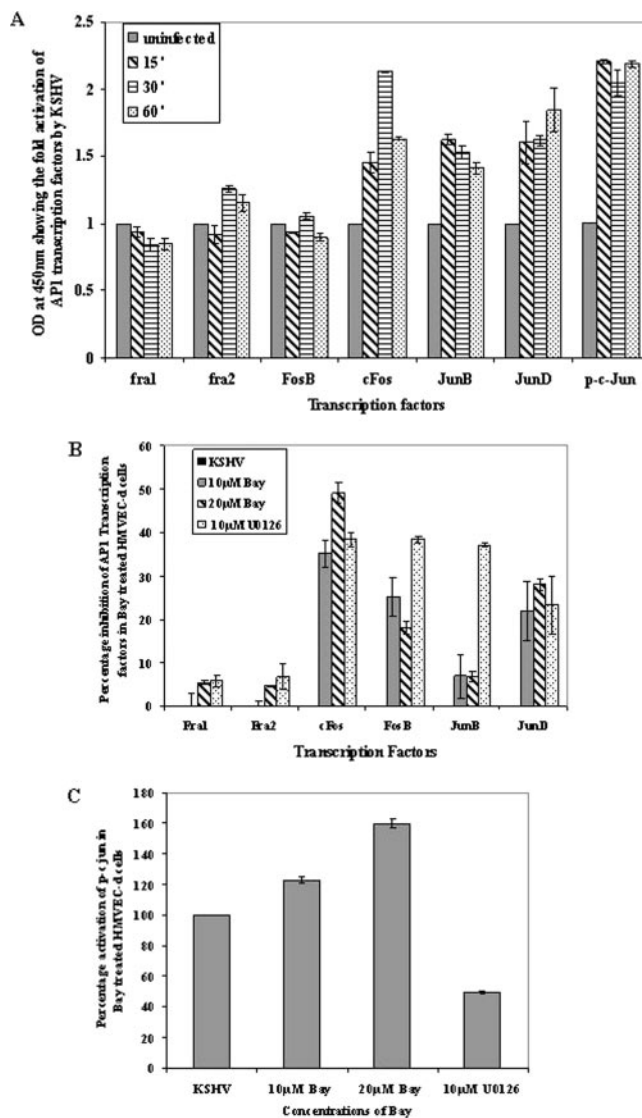

FIG. 8. Effect of NF-κB inhibition on AP-1 transcription factor activation. (A) Nuclear extracts prepared from uninfected HMVEC-d cells or HMVEC-d cells infected with KSHV for 15 min, 30 min, and 60 min were tested for the activation of AP-1-regulated transcription factors by incubating the nuclear extracts with the plate-immobilized oligonucleotides containing the AP-1 transcription factor-specific site, followed by ELISA with antibodies to the respective transcription factors. The histogram represents the activation levels of phospho-c-Jun, JunB, JunD, Fra1, Fra2, Fos-B, and c-Fos in the nuclear extracts from KSHV-infected HMVEC-d cells. The data represent the averages and standard deviations of three experiments, and the values shown here are after normalization with uninfected cells. (B) Histogram depicting the percent inhibition of DNA binding of AP-1 transcription factors in nuclear extracts from HMVEC-d cells pretreated with two different concentrations of Bay11-7082 and 10 μM U0126, followed by infection with KSHV. (C) Histogram depicting the percent activation of DNA binding of the phospho-c-Jun transcription factor in HMVEC-d nuclear extracts. Percent inhibition and percent activation were calculated with respect to the DNA binding activities in KSHV-infected HMVEC-d cells without Bay11-7082 pretreatment. The data represent the averages ± standard deviations of three experiments.
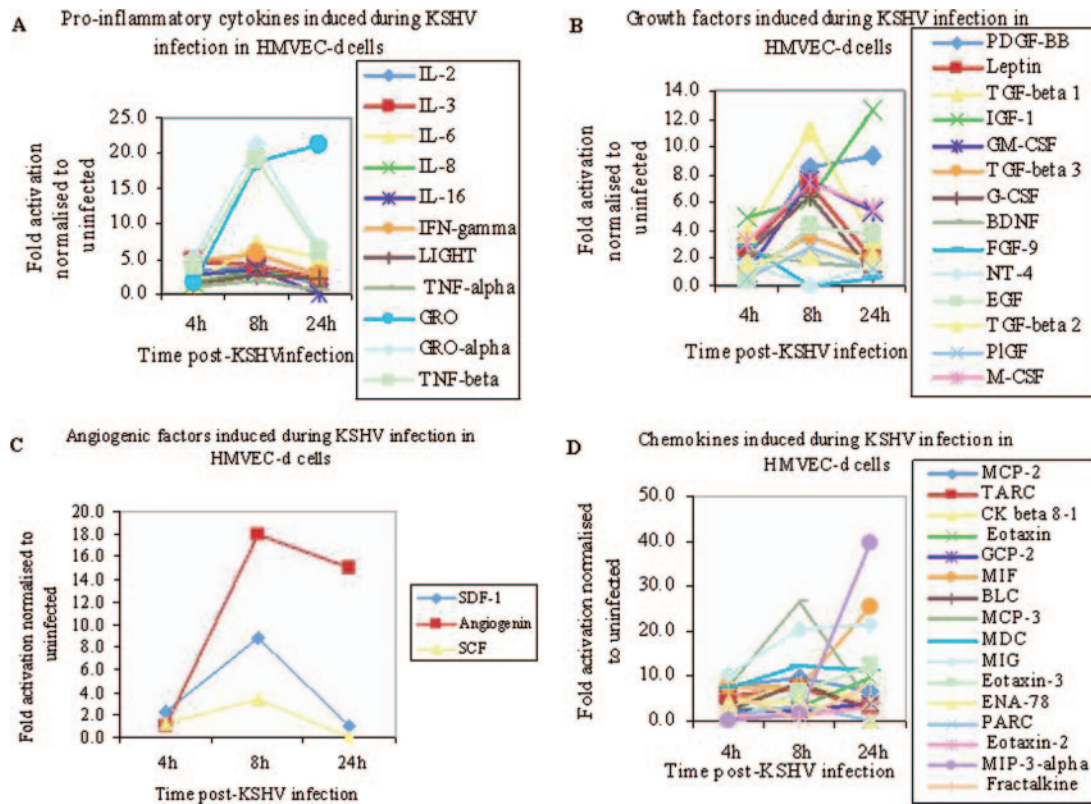
FIG. 9. Up regulation of proinflammatory cytokines, growth factors, angiogenic factors, and chemokines in HMVEC-d cells by KSHV. Densitometric analysis of cytokine array blots was carried out to determine the difference in the release of human cytokines from serum-starved, untreated HMVEC-d cells and KSHV-infected cells at three different time points. The values were normalized to identical background levels using the Ray Bio Human Cytokine antibody array V analysis tool. The increases in the cytokine levels were calculated by dividing the respective values obtained from infected-cell supernatants with the values obtained from uninfected-cell supernatants and cytokines showing significant change represented in a line graph format. (A) Proinflammatory cytokines, (B) growth factors, (C) angiogenic factors, and (D) chemokines that showed significant changes with respect to uninfected cells are represented in the graph.

activation of Fra1 and Fra2, whereas there was a very moderate effect of Bay11-7082 on JunB, with <20% inhibition (Fig. 8B). In contrast, Bay11-7082 displayed differential inhibitory effects on the activation of other AP-1 components (Fig. 8B). About 20% to 30% FosB and JunD inhibition was observed. The highest inhibition of >40 to 50% was observed for cFos with Bay11-7082. In contrast, phospho-c-Jun activation increased by about 23% and 60% with 10 μM and 20 μM Bay11-7082, respectively, over untreated cells infected with KSHV (Fig. 8C). Our previous studies have demonstrated that the MEK1/2 inhibitor U0126 prevented the activation of phospho-c-Jun by approximately 60% and that of cFos by 55% in HFF (57). Similarly, U0126, when used as a specificity control in this study, inhibited phospho-c-Jun, cFos, FosB, JunB, and JunD activities by about 55%, 40%, 41%, 42%, and 23%, respectively, and did not have any effect on Fra1 and Fra2 (Fig. 8B and C). These results indicate that NF-κB has differential impacts on the activation of the AP-1 family of transcription factors in KSHV-infected adherent target cells.

KSHV infection leads to NF-κB-mediated up regulation of cytokines. KS lesion is an inflammatory angioproliferative lesion characterized by the presence of a variety of inflammatory cells, proinflammatory cytokines, and angiogenic factors in the lesions (16). Cultured KS lesion spindle cells require cytokines

for their survival and proliferation (41), suggesting that cytokines probably act in both an autocrine and paracrine fashion. In our oligonucleotide array analysis of KSHV-infected HMVEC-d cells and HFF at 2 h and 4 h p.i., we observed the reprogramming of host transcriptional machinery regulating a variety of cellular processes, including apoptosis, cell cycle regulation, signaling, inflammatory response, and angiogenesis (46). Since NF-κB is known to regulate the majority of these factors, we next analyzed the role of KSHV-induced NF-κB in the regulation of the factors.

Conditioned media collected from KSHV-infected HMVEC-d cells at various time points p.i. were used to study the cytokine profile. Compared to the uninfected HMVEC-d cells, KSHV infection induced an increase in the secretion of the following categories of factors: (i) proinflammatory cytokines, such as interleukin 2 (IL-2), IL-3, IL-6, IL-8, IL-16, GRO, GROα, and gamma interferon (IFN-γ) (Fig. 9A and Table 1); (ii) anti-inflammatory cytokines, such as IL-4, IL-5, and IL-15 (Table 1); (iii) growth factors, such as platelet-derived growth factor (PDGF-BB), leptin, transforming growth factor β1 (TGF-β1), TGF-β3, IGF-1, granulocyte-macrophage colony-stimulating factor (GM-CSF), G-CSF, M-CSF, and epidermal growth factor (EGF) (Fig. 9B and Table 1); (iv) angiogenic factors, like

TABLE 1. Cytokines up regulated during KSHV infection of HMVEC-d cells[a]

Cytokine	Activation (n-fold)					
	KSHV (4 h)	Bay[b] + KSHV (4 h)	KSHV (8 h)	Bay + KSHV (8 h)	KSHV (24 h)	Bay + KSHV (24 h)
Proinflammatory cytokines						
IL-2	3.3	0.6	3.8	1.0	1.2	0.8
IL-3	4.6	1.2	4.2	1.7	2.2	1.7
IL-6	1.6	3.0	7.2	3.0	5.1	1.1
IL-8	1.6	2.9	3.4	2.8	2.0	2.8
IL-16	2.7	0.0	3.5	3.6	0.0	0.6
IL-1β	1.4	0.4	1.9	0.8	0.4	0.7
IL-12-p40	1.9	0.0	0.0	1.8	0.0	1.6
IL-1α	1.0	0.5	0.2	0.6	0.6	0.6
IL-7	1.8	2.2	1.9	2.0	2.3	2.1
IFN-γ	4.6	1.4	5.8	2.3	2.6	2.2
LIGHT	1.4	0.0	2.7	2.0	2.1	0.7
TNF-α	1.0	0.4	2.0	0.3	0.5	0.1
GRO	1.6	3.8	18.7	17.8	21.1	17.0
GRO-α	5.3	7.0	21.3	8.2	6.8	5.6
TNF-β	4.2	5.3	18.9	4.9	6.1	3.3
Anti-inflammatory cytokines						
IL-4	5.8	1.9	7.3	0.8	1.3	0.0
IL-5	2.0	1.0	6.0	0.0	0.0	0.0
IL-15	2.2	0.0	4.3	0.8	0.0	0.5
IL-10	0.3	2.4	2.6	2.8	2.3	2.6
IL-13	0.9	0.0	0.5	0.0	0.0	0.0
LIF	1.5	0.7	1.6	1.5	0.8	1.1
Growth factors						
PDGF-BB	2.0	0.0	8.6	7.8	9.3	7.1
Leptin	2.8	0.0	7.2	0.4	1.9	0.0
TGF-β1	3.9	0.3	11.1	0.3	3.5	0.0
IGF-1	5.0	5.2	6.2	4.7	12.6	3.6
GM-CSF	0.9	3.0	7.5	4.5	5.3	3.1
TGF-β3	1.3	0.9	3.5	2.1	1.9	1.7
G-CSF	2.3	0.7	6.4	2.1	0.9	0.0
BDNF	2.4	1.2	1.6	1.7	1.4	1.5
FGF-4	1.7	0.0	0.0	2.2	0.0	1.9
FGF-6	1.4	0.0	0.0	1.7	0.0	1.0
FGF-7	1.4	0.0	0.0	0.8	0.0	0.0
FGF-9	2.9	0.7	0.0	2.0	0.6	1.7
NT-4	1.7	0.0	0.1	2.2	1.6	1.7
EGF	0.3	4.1	4.2	4.6	3.7	4.5
TGF-β2	1.7	1.9	2.2	2.5	2.0	2.3
PIGF	0.6	1.2	2.7	3.0	1.3	2.9
M-CSF	3.2	9.0	7.4	8.2	5.7	7.5
GDNF	1.1	0.7	1.0	1.0	1.3	0.8
HGF	0.6	0.4	0.6	0.5	1.0	0.4
NT-3	1.2	1.9	0.0	4.3	3.0	2.0
Osteoprotegerin	1.5	0.7	1.6	1.4	1.2	1.2
Angiogenic factors						
SDF-1	2.2	0.0	8.8	0.5	1.1	0.0
Angiogenin	1.0	2.9	18.0	3.2	15.0	5.0
SCF	1.2	0.0	3.4	0.9	0.0	0.7
Oncostatin M	1.1	0.3	0.1	0.9	0.5	0.9
TPO	1.7	0.1	0.9	1.4	0.5	1.2
VEGF	1.5	0.4	1.5	1.0	0.7	1.0
Flt-3 Ligand	1.9	0.0	0.2	1.4	0.6	0.0
Chemokines						
MCP-2	7.7	2.8	9.7	2.8	6.5	2.1
TARC	5.2	0.0	7.1	0.1	3.2	0.0
CKβ 8-1	3.9	1.4	8.4	1.5	4.1	0.0
Eotaxin	2.3	1.0	3.1	2.3	9.4	0.0
GCP-2	2.3	0.0	2.2	1.8	3.9	0.0
MIF	7.8	1.5	7.3	7.2	25.2	3.3

Continued on following page

TABLE 1—*Continued*

Cytokine	Activation (*n*-fold)					
	KSHV (4 h)	Bay[b] + KSHV (4 h)	KSHV (8 h)	Bay + KSHV (8 h)	KSHV (24 h)	Bay + KSHV (24 h)
BLC	2.4	1.0	8.3	1.1	2.2	0.0
MCP-3	7.5	8.6	26.3	2.2	3.8	0.0
MDC	7.4	12.1	12.2	9.5	11.2	8.3
MIG	10.2	15.0	20.4	15.3	21.4	15.3
Eotaxin 3	0.0	1.7	6.6	4.4	12.1	0.2
ENA-78	4.1	2.4	4.2	2.5	0.2	1.9
PARC	1.1	0.0	3.5	1.4	0.0	0.7
Eotaxin 2	1.3	0.7	1.3	1.2	3.0	0.5
IP-10	1.4	0.3	1.0	1.1	0.5	0.8
MIP-3α	0.0	1.2	1.6	4.1	39.6	0.0
I-309	1.5	0.1	0.0	0.8	1.5	1.3
MCP-1	1.2	1.4	2.1	1.5	1.1	1.5
RANTES	0.9	0.2	0.8	0.5	1.0	0.5
MIP-1β	1.0	1.3	2.2	1.3	1.3	1.3
MIP-1δ	0.7	0.0	0.0	0.1	0.0	0.0
Fractalkine	6.1	9.0	0.6	10.5	8.1	9.0
NAP-2	0.6	0.5	0.5	0.5	0.9	0.4
Growth factor binding proteins						
IGFBP-2	0.9	0.7	2.6	0.8	1.3	0.4
IGFBP-1	0.6	0.5	0.6	0.6	0.9	0.4
IGFBP-3	1.4	0.8	0.0	1.4	0.8	1.3
IGFBP-4	1.9	0.0	0.7	3.5	0.3	2.3
Tissue inhibitors of matrix metalloproteinases						
TIMP-1	1.0	1.4	2.1	1.7	1.4	1.7
TIMP-2	1.1	1.7	2.9	2.1	1.5	2.0

[a] Conditioned media from cells infected with KSHV for 2 h, 8 h, and 24 h and cells pretreated with Bay11-7082, followed by infection with KSHV, were assayed using Ray Bio Human Cytokine antibody array V according to the manufacturer's instructions. The densitometric values were substituted in the Ray Bio Human Cytokine antibody array V analysis tool, and the total array values were normalized to the same background level. The cytokines were categorized into proinflammatory cytokines, anti-inflammatory cytokines, growth factors, angiogenic factors, chemokines, tissue inhibitors of matrix metalloproteinases, and growth factor binding proteins. The increases in the cytokine levels were calculated by dividing the respective values obtained from infected-cell supernatant, both untreated and Bay11-7082 treated, with the values obtained from uninfected-cell supernatant.

[b] Bay, Bay11-7082.

SDF-1, angiogenin, and SCF (Fig. 9C and Table 1); (v) chemokines, such as MCP-2, MCP-3, TARC, CKβ 8-1, eotaxin, eotaxin 3, GCP-2, MIF, MIG, MDC, ENA-78, and BLC (Fig. 9D and Table 1); and (vi) tissue inhibitors of matrix metalloproteinases, such as TIMP-1 and TIMP-2 (Table 1).

Further analyses of the activation kinetics of these factors revealed three distinct patterns of induction (Fig. 9 and Table 1). In pattern 1, factors such as IL-2, IL-16, IL-4, IL-5, IL-15, G-CSF, SDF-1, TARC, ENA-78, and leptin were induced at a significant level at 4 h p.i., reached maximum induction at 8 h p.i., and fell to the 4-h level or basal level at 24 h p.i. In pattern 2, several of the factors, like IL-6, IL-8, LIGHT, GRO, IL-10, GM-CSF, EGF, TGF-β2, angiogenin, and eotaxin 3, were induced at a significant level only at 8 h p.i. and continued to be induced even at 24 h p.i. Cytokines, such as IL-3, IFN-γ, GROα, TNF-β, PDGF-BB, TGF-β1, IGF-1, M-CSF, MCP-2, CKβ 8-1, eotaxin, GCP-2, MIF, BLC, MCP-3, MDC, and MIG, were secreted at all three time points tested, which could probably play a role in the constitutive activation of NF-κB and KSHV biology.

Many of the KSHV infection-induced cytokines, growth factors, and angiogenic factors were inhibited by 10 μM Bay11-7082 pretreatment (Table 1). We observed twofold and four-fold reductions in IL-6 induction at 8 h and 24 h p.i., respectively. IL-3, IL-2, GROα, and IFN-γ showed greater than twofold reduction after Bay11-7082 pretreatment. Similarly, the observed remarkable increase in IGF-1, PDGF-BB, leptin, TGF-β1, M-CSF, GM-CSF, and G-CSF growth factors after KSHV infection was also reduced by more than twofold with Bay11-7082. Among the chemokines, MCPs, MIG, MDC, MIP3α, TARC, CKβ 8-1, eotaxins, MIF, PARC, GCP-2, and BLC showed more than a threefold increase, and most of these chemokines were significantly reduced by NF-κB inhibition. Appreciable changes were not detected in the growth factor binding protein and tissue inhibitors of matrix metalloproteinase induction with Bay11-7082 pretreatment, whereas anti-inflammatory cytokines, like IL-4, IL-5, IL-10, and IL-15, showed more than twofold reduction with 10 μM Bay11-7082 pretreatment, in comparison to the supernatant from untreated cells infected with KSHV. We also observed the up regulation of a variety of angiogenic factors, such as angiogenin, SCF, SDF-1, and VEGF, and they were also inhibited by Bay11-7082 pretreatment. Since the genes encoding these wide ranges of cytokines secreted upon KSHV infection possess NF-κB binding sites in their promoter regions, their inhibition clearly demonstrated the role of KSHV-induced NF-κB in the regulation of these factors.
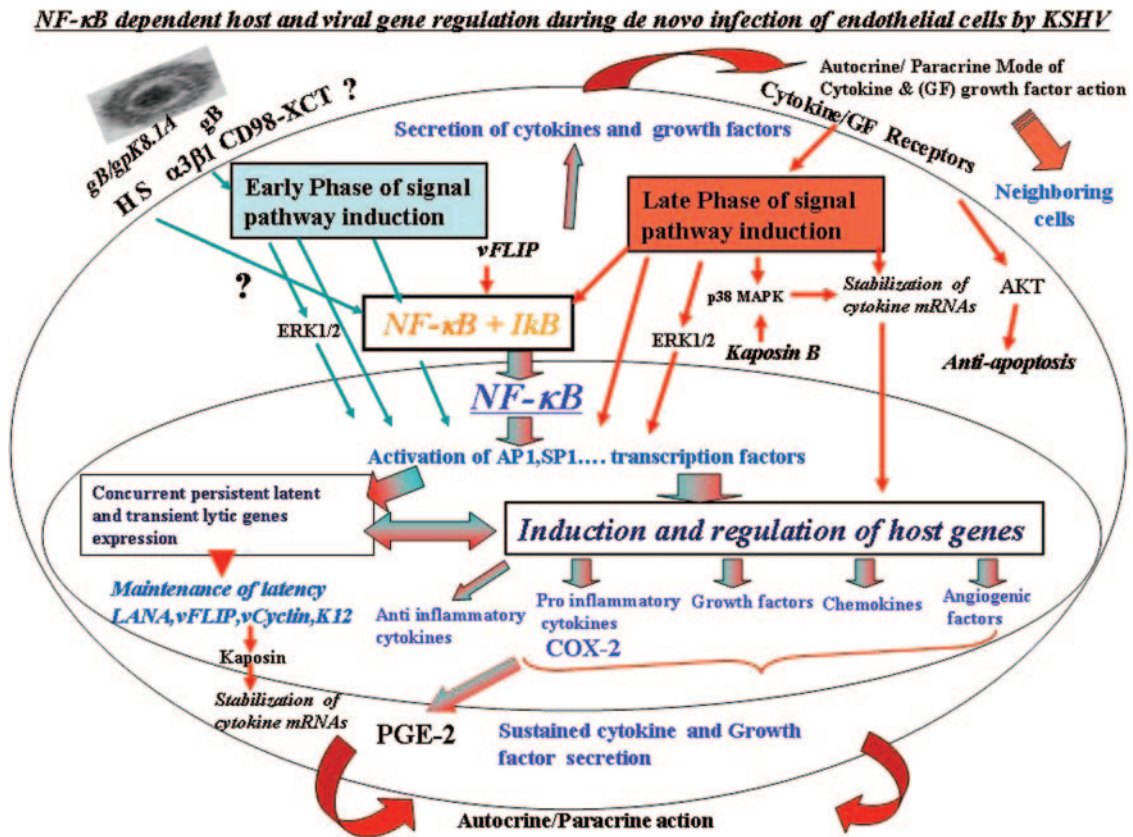
FIG. 10. Schematic representation depicting the early and late induction phases of NF-κB during in vitro KSHV infection of HMVEC-d cells and their potential roles in transcription factor regulation, establishment and maintenance of KSHV infection, and cytokine secretion. In the early phase of NF-κB induction (blue arrows), virus binding and entry lead to signal pathway induction, such as FAK, Src, PI 3-K, AKT, PKC-ζ, MAPK-ERK1/2, and NF-κB signal molecules. Activated NF-κB translocates into the nucleus, which coincides with viral-DNA entry into the infected-cell nuclei, concurrent transient expression of limited viral lytic genes, and persistent latent gene expression. Overlapping with these events, a limited number of cytokines and growth factors are induced, which is initiated by transcription factors, like AP-1 (induced by ERK1/2 and NF-κB). Early activation of NF-κB and ERK1/2 also leads to the activation and release of NF-κB-inducible host factors, which act in autocrine and paracrine fashions on the infected, as well as neighboring, cells. The autocrine action of these factors, along with viral gene expression, probably contributes to the second, or late, phase of signal pathway activation (red arrows), including sustained NF-κB activation and phosphorylation of p38 MAPK, ERK1/2, and AKT required for the maintenance of latency. The blue and red arrows together indicate pathways induced during both early and late phases of KSHV infection.

DISCUSSION

During infection of target cells leading to a productive lytic replicative cycle or to the establishment of latency in certain target cells, herpesviruses need to overcome several obstacles, like apoptosis; host intrinsic, innate, and adaptive immune responses; and transcriptional restrictions. These obstacles need to be counteracted not only during the early time of infection, but also during the entire time of latent infection. Establishment of latent infection during in vitro infection of primary human endothelial cells or fibroblasts by KSHV provides an opportunity to analyze the various complex interactions between viral and host factors and the potential mechanism of establishment and maintenance of latent infection. Our previous studies have revealed that to overcome the obstacles early during infection, even before de novo viral gene transcription and expression, KSHV has adopted an optimum strategy of manipulating the host cells' preexisting signal pathways via interactions with cell surface receptors (Fig. 10). KSHV binds to the adherent target cell surface heparan sulfate

molecule, to integrins, to the transporter CD98-xCT complex, and possibly to other molecules. This is followed by virus entry overlapping with the induction of preexisting host cell signal pathways, such as FAK, Src, PI 3-K, Rho-GTPases, PKC-ζ, and ERK1/2. In this report, we provide multiple comprehensive evidence to suggest that, in addition to the signal cascades, and in contrast to the differential induction of ERK1/2 and p38 MAPK molecules, KSHV infection also induces NF-κB very early during infection, which is sustained throughout the period of observation. Our studies give a snapshot of the complex events occurring early during infection of adherent target cells (Fig. 10). For clarity, we have summarized below these events and their potential implications on KSHV biology and pathogenesis.

Role of NF-κB in KSHV gene expression during endothelial cell infection. Several inhibitors have been shown to inhibit NF-κB activation at different levels, such as the prevention of IκB phosphorylation by Bay11-7082; blocking of IκB degradation by protease inhibitors, like MG132; or preventing the

nuclear translocation of NF-κB by CAPE or SN50. We used Bay11-7082, and not the protease inhibitors, as they might affect the Notch signaling pathway involved in KSHV pathogenesis (33). KSHV-induced NF-κB was blocked by Bay11-7082, and dose-response studies indicate that both HMVEC-d cells and HFF have varying sensitivities to the inhibitor. Similar variation with Bay11-7082 pretreatment was observed between HEK 293 cells and murine pre-B cells upon TNF-α treatment (22, 23).

We have previously demonstrated that KSHV-induced ERK1/2 play roles in the regulation of ORF 50 and ORF 73 gene expression, probably in the initiation of their expression. KSHV-induced NF-κB also appears to influence viral gene expression, which could be by direct interactions with the viral gene transcription initiation region or by indirect methods, such as the activation of host transcription factors and/or host genes, which in turn play roles in viral gene expression. Examination of ORF 50 and ORF 73 gene promoter regions show that only the ORF 50 gene, and not the ORF 73 gene, possesses NF-κB binding sites in its promoter region (35), suggesting that NF-κB could directly influence the transcriptional activation of the ORF 50 gene. KSHV latency-associated vFLIP has been shown to persistently activate NF-κB by interacting with the IKKα-IKKβ-IKKγ complex, and this has been taken as evidence for NF-κB's role in the maintenance of KSHV latency in PEL cells (13). However, how NF-κB regulates the latent genes is not known. ORF 50 (RTA) is believed to contribute to the establishment of latency through activation of LANA-1 expression in the early stages of infection (36). LANA-1 has been shown to physically interact with RBPJκ and to bind to the RTA promoter and block the activation of RTA (34). Thus, there exists a feedback loop through which LANA-1 and RTA possibly regulate each other. Even though there is no NF-κB binding site in the ORF 73 promoter, since the impact of blocking RTA could be manifested at various levels, the inhibition of ORF 73 gene expression by NF-κB inhibition could also be due to the blocking of RTA expression by Bay11-7082 pretreatment.

KSHV vIRF2 and K8 are expressed early during infection of HMVEC-d cells, and Bay11-7082 pretreatment inhibited the expression of these genes. Since RTA (ORF 50) protein is known to control the transcription of both K8 and vIRF2 by binding to the RTA response element present in the promoter regions of these lytic genes, K8 and vIRF2 inhibition upon NF-κB blockade could be attributed directly to RTA inhibition. The regulation of the lytic K5 gene is known to be independent of RTA (47) and was not influenced by ERK1/2 early during infection (27, 57). Since the K5 gene also does not have an NF-κB binding site, inhibition of the K5 gene observed after Bay11-7082 pretreatment could also be an indirect effect of various transcription factors under the control of NF-κB. Our results are in agreement with the studies by Keller et al. (27), who did not observe any increase in lytic gene activation in PEL cells after Bay11-7082 treatment.

KSHV induced NF-κB and AP-1 activation. Activation of any viral or cellular gene is not controlled by a single transcription factor but by interplay between various transcription factors, and one transcription factor could control the expression of others. It is interesting that the LANA-1 and K5 genes possess several transcription factor binding motifs, including

AP-1, SP1, cMyc, and c-Jun. Previous reports demonstrated that AP-1 activity may be critical for very early activation of the RTA and K8 promoters during the lytic cycle (75), and our studies have shown that ERK1/2, via the activation of AP-1 and other MAPK-related transcription factors, play important roles in the activation of the LANA-1 and RTA genes (57). Inhibition of ERK1/2 using the MEK inhibitor U0126 blocked RTA, LANA-1, K8, and vIRF2 gene expression but had minimal effect on K5 (57), whereas Bay11-7082 pretreatment inhibited all five of the genes. These studies demonstrate that KSHV gene expression is controlled by the regulation of multiple transcription factors, and inhibiting ERK1/2 probably inhibited only the factors downstream of ERK1/2. In contrast, Bay11-7082 pretreatment leads to the inhibition of both NF-κB and the AP-1 family of transcription factors, resulting in the blockade of all the viral genes tested. By inducing NF-κB and subsequent transcription factors, like AP-1, KSHV must overcome the transcription block in quiescent cells.

Rapid NF-κB activation is evident in KSHV-infected target cells. At nearly the same time, there is activation of the AP-1 family of transcription factors, accompanied by KSHV lytic gene expression. NF-κB could influence AP-1 transcription factors, which have κB binding sites in their promoters. We observed an appreciable increase in cFos, FosB, c-Jun, JunB, and JunD transcription factors after KSHV infection, and this activation was inhibited significantly by NF-κB inhibition (Fig. 8B). Downstream phosphorylation of AP-1 transcription factors was probably inhibited by NF-κB inhibition, clearly demonstrating that the regulation of AP-1 transcription factors could also be due to NF-κB.

The effect of NF-κB inhibition on AP-1 transcription factors could be at multiple levels: (i) it might affect gene transcription, as the AP-1 family of transcription factors are known to have a κB binding site in their promoters; (ii) it might affect the phosphorylation of transcription factors; and (iii) the DNA binding activity of transcription factors could also be inhibited. Further studies are needed to identify the mechanism of AP-1 down regulation by NF-κB inhibition.

Inhibition of KSHV-induced NF-κB and c-Jun activation. One of our surprising observations was that in cells pretreated with Bay11-7082 before KSHV infection, c-Jun was further up regulated, and there was a dose-dependent increase in c-Jun DNA binding activity. Generally, AP-1 complexes function as positive regulators of cell proliferation by regulating the expression of essential cell cycle proteins, such as D1, p53, p21, p19, and p16, and differential effects are also present among different members (60). Constitutive activation of c-Jun is known to induce apoptosis (54). In c-Jun knockout cells, there was an up regulation of NF-κB, and when c-Jun was ectopically expressed, NF-κB levels were reduced (53). The absence of NF-κB-mediated inhibition of JNK activation was known to contribute to TNF-α-induced apoptosis (67). This evidence clearly suggests that there is negative regulation between c-Jun and NF-κB. It is reasonable to speculate that the increase in c-Jun activation upon NF-κB inhibition could lead to an increase in latent and lytic gene activation. However, except c-Jun, all members of the AP-1 family of transcription factors were inhibited with NF-κB inhibition. Hence, it is evident that viral gene regulation is not controlled by a single transcription factor but instead by the involvement of a variety of transcrip-

tion factors. It is likely that KSHV activates c-Jun for the production of cytokines and lytic gene expression. Since hyperactivation of c-Jun may be deleterious for the cell, as it is proapoptotic, KSHV probably activates NF-κB to regulate c-Jun phosphorylation to allow the infected cells to survive.

Implications for sustained NF-κB induction by KSHV. The sustained induction of NF-κB during infection of endothelial cells in vivo is probably required to overcome apoptosis; host intrinsic, innate, and adaptive immune responses; and transcriptional restriction, not only during the early stages of infection, but also during the establishment and subsequent maintenance of latency. Activated NF-κB is known to be critical to escape immune system surveillance and to block apoptosis by directly binding to p53 and thus preventing p53 transcriptional activity; through competition for transcriptional coactivators, like CBP/p300 (24); by activating various antiapoptotic molecules; or by inducing the secretion of various cytokines. KSHV infection-induced sustained NF-κB activation probably performs all these functions.

Activation of transcription factors requires the phosphorylation of multiple upstream signaling molecules. Our previous studies have shown that KSHV induces multiple signaling pathways, which probably aids in the successful establishment of infection and the evasion of surveillance by the immune system (13, 44, 57). The initial binding event appears to be enough for the activation of NF-κB, and this early phase of activation (Fig. 10) could be due to both virus internalization and the expression of viral lytic genes, as many of the transiently expressed early viral lytic genes have roles in inducing NF-κB. During this phase, NF-κB probably induces proteins necessary for its sustained activation, and the later time point of activation could be due to the effect of antiapoptotic molecules and the secretion of cytokines, as many of these NF-κB-regulated cytokines are known to activate NF-κB (Fig. 10). NF-κB activation possibly leads to the induction of various antiapoptotic molecules, and NF-κB is in turn probably activated by the antiapoptotic KSHV latency-associated gene, like vFLIP, which was shown to be responsible for the constitutive activation of NF-κB in PEL cells (13). In addition to up regulating antiapoptotic proteins, NF-κB is known to induce signaling factors involved in the NF-κB activation pathway; by doing so, NF-κB probably ensures the constitutive expression of proteins necessary for its persistent activation in KSHV-infected endothelial cells.

Alternatively, Notch could also be responsible for the persistent activation of NF-κB, as Notch is known to augment NF-κB activity by retaining NF-κB in the nucleus (61). Activation of the Notch signal pathway by KSHV is known to be involved in the regulation of lytic gene expression (37). RBPJκ was shown to bind with RTA and to recruit it to its cognate recognition site, thus relieving the RBPJκ-mediated repression and up regulation of target gene expression. The upstream events leading to the activation of NF-κB, viral envelope glycoprotein, and the interacting receptor(s) involved in early induction are not known at present and are under study.

Activation of NF-κB by UV-KSHV demonstrated that virus binding and entry are enough to induce the activation of NF-κB in the early phase, and activation during the late phase could be due to a combination of vFLIP action and by the variety of cytokines and growth factors secreted from the infected cells. A recent report by Caselli et al. (9) showed that UV-treated virus could not activate NF-κB. This discrepancy may be due to technical reasons, such as the difference in virus titers. UV treatment of KSHV results in a reduction in viral copy numbers (presumably due to virus adhering to the plastic). Hence, it is necessary to treat the virus with DNase and estimate the copy numbers after UV treatment and to utilize copy numbers similar to those of live KSHV.

ERK1/2, p38 MAPK, and AKT induction by KSHV. ERK1/2 phosphorylation was critical for the initiation of KSHV latent and lytic gene expression (57). Our long-term activation study demonstrates biphasic activation kinetics of ERK1/2. The high level of early-phase ERK1/2 activation coincided with NF-κB activation, which could be attributed to virus binding and entry. The late phase of ERK1/2 activation was seen at 24 h p.i., which coincided with LANA-1 expression, indicating that the second phase could be due to the establishment of latency in these cells, as blocking ERK is known to inhibit LANA-1 expression (57). LANA-1 up regulates vIL-6 expression by inducing AP-1 transcription factors, which are known to be activated by the MAPK pathway (3, 77). Biphasic MAPK activation is also seen in other viruses, with the second phase coinciding with viral genome synthesis (26, 29, 38, 51). We have previously demonstrated that activation of the AP-1 and MAPK families of transcription factors via ERK1/2 is critical for latent and lytic gene expression (57). Hence, it is possible that the c-Jun phosphorylation we observed after NF-κB inhibition could also be due to ERK phosphorylation, which remains unaffected by Bay11-7082 pretreatment, whereas the requirement for multiple transcription factors for viral gene expression cannot be ruled out.

Besides the sustained NF-κB activation and biphasic ERK1/2 activation, we observed a late-time-point activation of p38 MAPK, which was in agreement with the result observed in our previous study (44). Kaposin B is known to induce the p38/MK2 pathway and to stabilize cytokine mRNAs (40). Unlike ERK1/2 and NF-κB, p38 MAPK is not activated by KSHV binding to target cells; instead, the activation was seen only after 8 h p.i. The p38 MAPK pathway is normally activated by stress, growth factors, and cytokines, resulting in proliferation, differentiation, development, and inflammation. Hence, KSHV-induced activation of NF-κB early during infection is probably necessary for cytokine release, and it is probably sustained by the activation of p38 MAPK during the later time period of latent infection (Fig. 10). Combined activation of both the MAPK pathway and the NF-κB pathway has been shown to be necessary for COX-2 induction and prostacyclin release in endothelial cells (66), and we have observed rapid sustained induction of COX-2 in KSHV-infected endothelial cells (59). Taken together, this suggests that the signal pathways may cooperate and induce the secretion of the cytokines, chemokines, and growth factors (Fig. 10).

COX-2 expression is known to be mediated through AKT via the NF-κB pathway (62). AKT is a survival signal molecule that is activated during many viral infections (25, 50, 68). We observed a triphasic activation of AKT in both target cells. The initial activation could have been due to virus binding and entry, and the second phase could be due to viral gene expression. KSHV interaction with target cells induced PI 3-K during the early stages of infection (44). AKT is the immediate down-

stream signaling molecule of PI 3-K; hence, virus binding to integrin could have initiated the AKT phosphorylation. Induction of lytic genes could have contributed to the second phase of activation. The variety of growth factors and cytokines induced at the later time points could act both in paracrine and autocrine fashions to stimulate the third phase of PI3K/AKT pathway activation. In summary, these results suggest that in adherent target cells, KSHV induces the differential activation of various signaling molecules but sustains the activation of NF-κB to modulate various transcription factors responsible for latent and lytic gene regulation.

Implications of KSHV-induced NF-κB and induction of cytokines. The role played by NF-κB in regulating cytokines, like IL-8, IL-6, GROα, IL-1β, IFN-γ, and VEGF, in PEL cells is well documented (4, 39, 52, 74). Our studies clearly demonstrated that KSHV infection of primary endothelial cells leads to the increased secretion of human cytokines, chemokines, and growth factors via the activation of NF-κB. Among the strongest up regulated host molecules on the array were cytokines and chemokines, like GROα, IL-2, IL-3, IL-4, IL-6, IL-8, IFN-γ, GM-CSF, PDGF, IGF-1, eotaxin, MCPs, MIF, and angiogenin. Among these, GRO, IL-2, IL-6, IL-8, IFN-γ, GM-CSF, PDGF, IGF, and MCP genes are well-established target genes of NF-κB (48). Except for a few cytokines, growth factors, chemokines, and angiogenic factors that were modulated by KSHV infection at all three time points, we observed that there were many cytokines that were released only at one or two time points, thus suggesting that KSHV may be selectively regulating these factors for its advantage. Further studies are essential to define the variations in KSHV-induced cytokines.

Several lines of evidence demonstrate that KSHV is etiologically associated with KS pathogenesis (12). Expression of limited KSHV latent proteins, such as LANA-1, vFLIP, vCyclin D, kaposins, and the lytic protein K5, has been detected in the KS lesion endothelial cells, and lytic cycle proteins have been detected in the limited percentage of KS lesion-associated inflammatory cells (20). KS tumorigenesis appears to require an ongoing lytic infection, since interruption of lytic replication by drugs such as ganciclovir appears to prevent KS development (10). KSHV latent gene products, such as vFLIP, acting on NF-κB in latently infected endothelial cells and lytic infection in inflammatory cells expressing vGPCR, vIL-2, vMIPs, etc., could collectively contribute to the initiation and maintenance of the KS lesion-associated inflammatory microenvironment. Our observation of a robust induction of cytokines, growth factors, and angiogenic factors by KSHV at 4 h, 8 h, and 24 h p.i. of endothelial cells (46), together with our demonstration of sustained activation of NF-κB, a key inflammatory induction molecule, suggests that primary infection of endothelial cells could also create the microenvironment observed in the KS lesions. The persistent NF-κB activation by KSHV could be mediated by a combination of viral latent genes, like vFLIP expression in the endothelial cells, and by the cytokines and growth factors secreted in the infected-cell supernatant (50).

The model that emerges from our current and previous studies is that primary infection of endothelial cells by KSHV initiates the host cell cytokine and growth factor cascades, which are probably subsequently maintained by the interplay between viral and host genes, and KSHV utilizes these cyto-

kines and growth factors for its own advantage, such as for the maintenance of latent infection and immune evasion (Fig. 10). The variety of cytokines and growth factors seen during KSHV primary infection of endothelial cells in our studies are strikingly similar to the cytokines and growth factors detected in the KS lesions. Although KSHV codes for several cytokines and chemokines that are known to activate NF-κB, none of them has been shown to be expressed in the latently infected KS lesion endothelial cells (55). It is possible that NF-κB, COX-2, PGE2, and other cytokines induced during in vivo infection of endothelial cells could be responsible for the growth factors and cytokines seen in the microenvironment of KS lesions. A recent study by Grossmann et al. (18) showed that the activation of NF-κB by vFLIP is required for the spindle shape of virus-infected endothelial cells, which contributes to their cytokine release. Activation of several cytokines and growth factors in our study could be attributed to multiple viral proteins, apart from vFLIP.

The establishment of latency by KSHV is a very complex process, and no single viral or host gene, transcription factor, signal molecule, or cytokine activation could independently be responsible for it. Instead, it is probably mediated by a combination of all these factors selected over the time of evolution of KSHV along with the host. Hence, the outcome of in vitro KSHV infection of HMVEC-d cells and, by analogy, the in vivo infection of endothelial cells probably represents a complex interplay between host cell signal molecules, cytokines, growth factors, transcription factors, and viral latent gene products resulting in an equilibrium state in which virus maintains its latency, blocks apoptosis, blocks host cell intrinsic and innate responses, and escapes from the host adaptive immune responses (Fig. 10). KSHV probably utilizes NF-κB, COX-2, and other host cell factors, including the inflammatory factors, for its advantage, such as the establishment of latent infection and immune modulation. However, the combination of factors, such as the absence of immune regulation, an unchecked KSHV lytic cycle, and increased virus load, resulting in widespread KSHV infection of endothelial cells, leading to induction of inflammatory cytokines and growth factors, and the inability of the host to modulate this inflammation may contribute to KSHV-induced KS lesions. Thus, it is possible that effective inhibition of inflammatory responses, including NF-κB, COX-2, and PGE2, could lead to reduced latent KSHV infection of endothelial cells, which may in turn lead to a reduction in the accompanying inflammation and KS lesions.

REFERENCES

1. **Akula, S. M., N. P. Pramod, F. Z. Wang, and B. Chandran.** 2001. Human herpesvirus 8 envelope-associated glycoprotein B interacts with heparan sulfate-like moieties. Virology **284:**235–249.
2. **Akula, S. M., F. Z. Wang, J. Vieira, and B. Chandran.** 2001. Human herpesvirus 8 interaction with target cells involves heparan sulfate. Virology **282:**245–255.
3. **An, J., A. K. Lichtenstein, G. Brent, and M. B. Rettig.** 2002. The Kaposi sarcoma-associated herpesvirus (KSHV) induces cellular interleukin 6 expression: role of the KSHV latency-associated nuclear antigen and the AP1 response element. Blood **99:**649–654.

4. **An, J., Y. Sun, R. Sun, and M. B. Rettig.** 2003. Kaposi's sarcoma-associated herpesvirus encoded vFLIP induces cellular IL-6 expression: the role of the NF-κB and JNK/AP1 pathways. Oncogene **22:**3371–3385.

5. **Baeuerle, P. A., and D. Baltimore.** 1996. NF-kappa B: ten years after. Cell **87:**13–20.

6. **Baldwin, A. S., Jr.** 1996. The NF-kappa B and I kappa B proteins: new discoveries and insights. Annu. Rev. Immunol. **14:**649–683.

7. **Bechtel, J. T., R. C. Winant, and D. Ganem.** 2005. Host and viral proteins in the virion of Kaposi's sarcoma-associated herpesvirus. J. Virol. **79:**4952–4964.

8. **Cahir-McFarland, E. D., K. Carter, A. Rosenwald, J. M. Giltnane, S. E. Henrickson, L. M. Staudt, and E. Kieff.** 2004. Role of NF-κB in cell survival and transcription of latent membrane protein 1-expressing or Epstein-Barr virus latency III-infected cells. J. Virol. **78:**4108–4119.

9. **Caselli, E., S. Fiorentini, C. Amici, D. Di Luca, A. Caruso, and M. G. Santoro.** 30 November 2006, posting date. Human herpesvirus 8 acute infection of endothelial cells induces monocyte chemoattractant protein 1-dependent capillary-like structure formation: role of the IKK/NF-κB pathway. Blood. doi:10.1182/ blood.2006–03-012500.

10. **Casper, C., W. G. Nichols, M. L. Huang, L. Corey, and A. Wald.** 2004. Remission of HHV-8 and HIV-associated multicentric Castleman disease with ganciclovir treatment. Blood **103:**1632–1634.

11. **Cesarman, E., Y. Chang, P. S. Moore, J. W. Said, and D. M. Knowles.** 1995. Kaposi's sarcoma-associated herpesvirus-like DNA sequences in AIDS-related body-cavity-based lymphomas. N. Engl. J. Med. **332:**1186–1191.

12. **Chang, Y., E. Cesarman, M. S. Pessin, F. Lee, J. Culpepper, D. M. Knowles, and P. S. Moore.** 1994. Identification of herpesvirus-like DNA sequences in AIDS-associated Kaposi's sarcoma. Science **266:**1865–1869.

13. **Chaudhary, P. M., A. Jasmin, M. T. Eby, and L. Hood.** 1999. Modulation of the NF-kappa B pathway by virally encoded death effector domains-containing proteins. Oncogene **18:**5738–5746.

14. **Coscoy, L., and D. Ganem.** 2001. A viral protein that selectively downregulates ICAM-1 and B7-2 and modulates T cell costimulation. J. Clin. Investig. **107:**1599–1606.

15. **Dourmishev, L. A., A. L. Dourmishev, D. Palmeri, R. A. Schwartz, and D. M. Lukac.** 2003. Molecular genetics of Kaposi's sarcoma-associated herpesvirus (human herpesvirus-8) epidemiology and pathogenesis. Microbiol. Mol. Biol. Rev. **67:**175–212.

16. **Ensoli, B., and R. C. Gallo.** 1995. AIDS-associated Kaposi's sarcoma: a new perspective of its pathogenesis and treatment. Proc. Assoc. Am. Physicians **107:**8–18.

17. **Ganem, D.** 1997. KSHV and Kaposi's sarcoma: the end of the beginning? Cell **91:**157–160.

18. **Grossmann, C., S. Podgrabinska, M. Skobe, and D. Ganem.** 2006. Activation of NF-κB by the latent vFLIP gene of Kaposi's sarcoma-associated herpesvirus is required for the spindle shape of virus-infected endothelial cells and contributes to their proinflammatory phenotype. J. Virol. **80:**7179–7185.

19. **Hammarskjold, M. L., and M. C. Simurda.** 1992. Epstein-Barr virus latent membrane protein transactivates the human immunodeficiency virus type 1 long terminal repeat through induction of NF-kappa B activity. J. Virol. **66:**6496–6501.

20. **Haque, M., K. Ueda, K. Nakano, Y. Hirata, C. Parravicini, M. Corbellino, and K. Yamanishi.** 2001. Major histocompatibility complex class I molecules are down-regulated at the cell surface by the K5 protein encoded by Kaposi's sarcoma-associated herpesvirus/human herpesvirus-8. J. Gen. Virol. **82:**1175–1180.

21. **Hayden, M. S., and S. Ghosh.** 2004. Signaling to NF-κB. Genes Dev. **18:**2195–2224.

22. **Huang, T. T., S. L. Feinberg, S. Suryanarayanan, and S. Miyamoto.** 2002. The zinc finger domain of NEMO is selectively required for NF-kappa B activation by UV radiation and topoisomerase inhibitors. Mol. Cell. Biol. **22:**5813–5825.

23. **Hung, J. H., I. J. Su, H. Y. Lei, H. C. Wang, W. C. Lin, W. T. Chang, W. Huang, W. C. Chang, Y. S. Chang, C. C. Chen, and M. D. Lai.** 2004. Endoplasmic reticulum stress stimulates the expression of cyclooxygenase-2 through activation of NF-κB and pp38 mitogen-activated protein kinase. J. Biol. Chem. **279:**46384–46392.

24. **Ikeda, A., X. Sun, Y. Li, Y. Zhang, R. Eckner, T. S. Doi, T. Takahashi, Y. Obata, K. Yoshioka, and K. Yamamoto.** 2000. p300/CBP-dependent and -independent transcriptional interference between NF-κB RelA and p53. Biochem. Biophys. Res. Commun. **272:**375–379.

25. **Jeong, S. J., C. A. Pise-Masison, M. F. Radonovich, H. U. Park, and J. N. Brady.** 2005. Activated AKT regulates NF-κB activation, p53 inhibition and cell survival in HTLV-1-transformed cells. Oncogene **24:**6719–6728.

26. **Jiang, S. J., T. M. Lin, G. Y. Shi, H. L. Eng, H. Y. Chen, and H. L. Wu.** 2004. Inhibition of bovine herpesvirus-4 replication by arsenite through downregulation of the extracellular signal-regulated kinase signaling pathway. J. Biomed. Sci. **11:**500–510.

27. **Keller, S. A., D. Hernandez-Hopkins, J. Vider, V. Ponomarev, E. Hyjek, E. J. Schattner, and E. Cesarman.** 2006. NF-κB is essential for the progression of KSHV- and EBV-infected lymphomas in vivo. Blood **107:**3295–3302.

28. **Keller, S. A., E. J. Schattner, and E. Cesarman.** 2000. Inhibition of NF-κB

29. induces apoptosis of KSHV-infected primary effusion lymphoma cells. Blood **96:**2537–2542.

29. **Kim, S. M., E. J. Kim, S. I. Park, and J. H. Nam.** 2005. The role of ERK1/2 activation in the infection of HeLa cells with human coxsackievirus B3. Acta Virol. **49:**91–96.

30. **Krishnan, H. H., P. P. Naranatt, M. S. Smith, L. Zeng, C. Bloomer, and B. Chandran.** 2004. Concurrent expression of latent and a limited number of lytic genes with immune modulation and antiapoptotic function by Kaposi's sarcoma-associated herpesvirus early during infection of primary endothelial and fibroblast cells and subsequent decline of lytic gene expression. J. Virol. **78:**3601–3620.

31. **Krishnan, H. H., N. Sharma-Walia, D. N. Streblow, P. P. Naranatt, and B. Chandran.** 2006. Focal adhesion kinase is critical for entry of Kaposi's sarcoma-associated herpesvirus into target cells. J. Virol. **80:**1167–1180.

32. **Laherty, C. D., H. M. Hu, A. W. Opipari, F. Wang, and V. M. Dixit.** 1992. The Epstein-Barr virus LMP1 gene product induces A20 zinc finger protein expression by activating nuclear factor kappa B. J. Biol. Chem. **267:**24157–24160.

33. **Lan, K., T. Choudhuri, M. Murakami, D. A. Kuppers, and E. S. Robertson.** 2006. Intracellular activated Notch1 is critical for proliferation of Kaposi's sarcoma-associated herpesvirus-associated B-lymphoma cell lines in vitro. J. Virol. **80:**6411–6419.

34. **Lan, K., D. A. Kuppers, and E. S. Robertson.** 2005. Kaposi's sarcoma-associated herpesvirus reactivation is regulated by interaction of latency-associated nuclear antigen with recombination signal sequence-binding protein Jκ, the major downstream effector of the Notch signaling pathway. J. Virol. **79:**3468–3478.

35. **Lan, K., D. A. Kuppers, S. C. Verma, and E. S. Robertson.** 2004. Kaposi's sarcoma-associated herpesvirus-encoded latency-associated nuclear antigen inhibits lytic replication by targeting Rta: a potential mechanism for virus-mediated control of latency. J. Virol. **78:**6585–6594.

36. **Lan, K., D. A. Kuppers, S. C. Verma, N. Sharma, M. Murakami, and E. S. Robertson.** 2005. Induction of Kaposi's sarcoma-associated herpesvirus latency-associated nuclear antigen by the lytic transactivator RTA: a novel mechanism for establishment of latency. J. Virol. **79:**7453–7465.

37. **Liang, Y., and D. Ganem.** 2003. Lytic but not latent infection by Kaposi's sarcoma-associated herpesvirus requires host CSL protein, the mediator of Notch signaling. Proc. Natl. Acad. Sci. USA **100:**8490–8495.

38. **Luo, H., B. Yanagawa, J. Zhang, Z. Luo, M. Zhang, M. Esfandiarei, C. Carthy, J. E. Wilson, D. Yang, and B. M. McManus.** 2002. Coxsackievirus B3 replication is reduced by inhibition of the extracellular signal-regulated kinase (ERK) signaling pathway. J. Virol. **76:**3365–3373.

39. **Matta, H., R. M. Surabhi, J. Zhao, V. Punj, Q. Sun, S. Schamus, L. Mazzacurati, and P. M. Chaudhary.** 28 August 2006, posting date. Induction of spindle cell morphology in human vascular endothelial cells by human herpesvirus 8-encoded viral FLICE inhibitory protein K13. Oncogene. doi: 10.1038/sj.onc.1209931.

40. **McCormick, C., and D. Ganem.** 2005. The kaposin B protein of KSHV activates the p38/MK2 pathway and stabilizes cytokine mRNAs. Science **307:**739–741.

41. **Miles, S. A., A. R. Rezai, J. F. Salazar-Gonzalez, M. Vander Meyden, R. H. Stevens, D. M. Logan, R. T. Mitsuyasu, T. Taga, T. Hirano, T. Kishimoto, et al.** 1990. AIDS Kaposi sarcoma-derived cells produce and respond to interleukin 6. Proc. Natl. Acad. Sci. USA **87:**4068–4072.

42. **Miyamoto, S., P. J. Chiao, and I. M. Verma.** 1994. Enhanced I kappa B alpha degradation is responsible for constitutive NF-kappa B activity in mature murine B-cell lines. Mol. Cell. Biol. **14:**3276–3282.

43. **Mocarski, E. S., Jr.** 1997. Propagating Kaposi's sarcoma-associated herpesvirus. N. Engl. J. Med. **336:**214–215.

44. **Naranatt, P. P., S. M. Akula, C. A. Zien, H. H. Krishnan, and B. Chandran.** 2003. Kaposi's sarcoma-associated herpesvirus induces the phosphatidylinositol 3-kinase-PKC-zeta-MEK-ERK signaling pathway in target cells early during infection: implications for infectivity. J. Virol. **77:**1524–1539.

45. **Naranatt, P. P., H. H. Krishnan, M. S. Smith, and B. Chandran.** 2005. Kaposi's sarcoma-associated herpesvirus modulates microtubule dynamics via RhoA-GTP-diaphanous 2 signaling and utilizes the dynein motors to deliver its DNA to the nucleus. J. Virol. **79:**1191–1206.

46. **Naranatt, P. P., H. H. Krishnan, S. R. Svojanovsky, C. Bloomer, S. Mathur, and B. Chandran.** 2004. Host gene induction and transcriptional reprogramming in Kaposi's sarcoma-associated herpesvirus (KSHV/HHV-8)-infected endothelial, fibroblast, and B cells: insights into modulation events early during infection. Cancer Res. **64:**72–84.

47. **Okuno, T., Y. B. Jiang, K. Ueda, K. Nishimura, T. Tamura, and K. Yamanishi.** 2002. Activation of human herpesvirus 8 open reading frame K5 independent of ORF50 expression. Virus Res. **90:**77–89.

48. **Pahl, H. L.** 1999. Activators and target genes of Rel/NF-κB transcription factors. Oncogene **18:**6853–6866.

49. **Pan, H., J. Xie, F. Ye, and S. J. Gao.** 2006. Modulation of Kaposi's sarcoma-associated herpesvirus infection and replication by MEK/ERK, JNK, and p38 multiple mitogen-activated protein kinase pathways during primary infection. J. Virol. **80:**5371–5382.

50. **Pati, S., M. Cavrois, H. G. Guo, J. S. Foulke, Jr., J. Kim, R. A. Feldman, and**

M. Reitz. 2001. Activation of NF-κB by the human herpesvirus 8 chemokine receptor ORF74: evidence for a paracrine model of Kaposi's sarcoma pathogenesis. J. Virol. 75:8660–8673.

51. Pleschka, S., T. Wolff, C. Ehrhardt, G. Hobom, O. Planz, U. R. Rapp, and S. Ludwig. 2001. Influenza virus propagation is impaired by inhibition of the Raf/MEK/ERK signalling cascade. Nat. Cell Biol. 3:301–305.

52. Polson, A. G., D. Wang, J. DeRisi, and D. Ganem. 2002. Modulation of host gene expression by the constitutively active G protein-coupled receptor of Kaposi's sarcoma-associated herpesvirus. Cancer Res. 62:4525–4530.

53. Sanchez-Perez, I., S. A. Benitah, M. Martinez-Gomariz, J. C. Lacal, and R. Perona. 2002. Cell stress and MEKK1-mediated c-Jun activation modulate NFκB activity and cell viability. Mol. Biol. Cell. 13:2933–2945.

54. Sanchez-Perez, I., and R. Perona. 1999. Lack of c-Jun activity increases survival to cisplatin. FEBS Lett. 453:151–158.

55. Schulz, T. F. 1998. Kaposi's sarcoma-associated herpesvirus (human herpesvirus-8). J. Gen. Virol. 79:1573–1591.

56. Schulz, T. F., J. Sheldon, and J. Greensill. 2002. Kaposi's sarcoma associated herpesvirus (KSHV) or human herpesvirus 8 (HHV8). Virus Res. 82:115–126.

57. Sharma-Walia, N., H. H. Krishnan, P. P. Naranatt, L. Zeng, M. S. Smith, and B. Chandran. 2005. ERK1/2 and MEK1/2 induced by Kaposi's sarcoma-associated herpesvirus (human herpesvirus 8) early during infection of target cells are essential for expression of viral genes and for establishment of infection. J. Virol. 79:10308–10329.

58. Sharma-Walia, N., P. P. Naranatt, H. H. Krishnan, L. Zeng, and B. Chandran. 2004. Kaposi's sarcoma-associated herpesvirus/human herpesvirus 8 envelope glycoprotein gB induces the integrin-dependent focal adhesion kinase-Src-phosphatidylinositol 3-kinase-rho GTPase signal pathways and cytoskeletal rearrangements. J. Virol. 78:4207–4223.

59. Sharma-Walia, N., H. Raghu, S. Sadagopan, R. Sivakumar, M. V. Veettil, P. P. Naranatt, M. M. Smith, and B. Chandran. 2006. Cyclooxygenase 2 induced by Kaposi's sarcoma-associated herpesvirus early during in vitro infection of target cells plays a role in the maintenance of latent viral gene expression. J. Virol. 80:6534–6552.

60. Shaulian, E., and M. Karin. 2002. AP-1 as a regulator of cell life and death. Nat. Cell Biol. 4:E131–E136.

61. Shin, H. M., L. M. Minter, O. H. Cho, S. Gottipati, A. H. Fauq, T. E. Golde, G. E. Sonenshein, and B. A. Osborne. 2006. Notch1 augments NF-κB activity by facilitating its nuclear retention. EMBO J. 25:129–138.

62. St-Germain, M. E., V. Gagnon, S. Parent, and E. Asselin. 2004. Regulation of COX-2 protein expression by Akt in endometrial cancer cells is mediated through NF-κB/IκB pathway. Mol. Cancer. 3:7.

63. Staskus, K. A., W. Zhong, K. Gebhard, B. Herndier, H. Wang, R. Renne, J. Beneke, J. Pudney, D. J. Anderson, D. Ganem, and A. T. Haase. 1997. Kaposi's sarcoma-associated herpesvirus gene expression in endothelial (spindle) tumor cells. J. Virol. 71:715–719.

64. Sun, Q., H. Matta, G. Lu, and P. M. Chaudhary. 2006. Induction of IL-8 expression by human herpesvirus 8 encoded vFLIP K13 via NF-κB activation. Oncogene 25:2717–2726.

65. Sun, R., S. F. Lin, K. Staskus, L. Gradoville, E. Grogan, A. Haase, and G.

66. Miller. 1999. Kinetics of Kaposi's sarcoma-associated herpesvirus gene expression. J. Virol. 73:2232–2242.

66. Syeda, F., J. Grosjean, R. A. Houliston, R. J. Keogh, T. D. Carter, E. Paleolog, and C. P. Wheeler-Jones. 2006. Cyclooxygenase-2 induction and prostacyclin release by protease-activated receptors in endothelial cells require cooperation between mitogen-activated protein kinase and NF-κB pathways. J. Biol. Chem. 281:11792–11804.

67. Tang, F., G. Tang, J. Xiang, Q. Dai, M. R. Rosner, and A. Lin. 2002. The absence of NF-κB-mediated inhibition of c-Jun N-terminal kinase activation contributes to tumor necrosis factor alpha-induced apoptosis. Mol. Cell. Biol. 22:8571–8579.

68. Thomas, K. W., M. M. Monick, J. M. Staber, T. Yarovinsky, A. B. Carter, and G. W. Hunninghake. 2002. Respiratory syncytial virus inhibits apoptosis and induces NF-kappa B activity through a phosphatidylinositol 3-kinase-dependent pathway. J. Biol. Chem. 277:492–501.

69. Thornburg, N. J., W. Kulwichit, R. H. Edwards, K. H. Shair, K. M. Bendt, and N. Raab-Traub. 2006. LMP1 signaling and activation of NF-κB in LMP1 transgenic mice. Oncogene 25:288–297.

70. Tomescu, C., W. K. Law, and D. H. Kedes. 2003. Surface downregulation of major histocompatibility complex class I, PE-CAM, and ICAM-1 following de novo infection of endothelial cells with Kaposi's sarcoma-associated herpesvirus. J. Virol. 77:9669–9684.

71. Vieira, J., P. O'Hearn, L. Kimball, B. Chandran, and L. Corey. 2001. Activation of Kaposi's sarcoma-associated herpesvirus (human herpesvirus 8) lytic replication by human cytomegalovirus. J. Virol. 75:1378–1386.

72. Wang, F. Z., S. M. Akula, N. P. Pramod, L. Zeng, and B. Chandran. 2001. Human herpesvirus 8 envelope glycoprotein K8.1A interaction with the target cells involves heparan sulfate. J. Virol. 75:7517–7527.

73. Wang, F. Z., S. M. Akula, N. Sharma-Walia, L. Zeng, and B. Chandran. 2003. Human herpesvirus 8 envelope glycoprotein B mediates cell adhesion via its RGD sequence. J. Virol. 77:3131–3147.

74. Wang, H. W., M. W. Trotter, D. Lagos, D. Bourboulia, S. Henderson, T. Makinen, S. Elliman, A. M. Flanagan, K. Alitalo, and C. Boshoff. 2004. Kaposi sarcoma herpesvirus-induced cellular reprogramming contributes to the lymphatic endothelial gene expression in Kaposi sarcoma. Nat. Genet. 36:687–693.

75. Wang, S. E., F. Y. Wu, H. Chen, M. Shamay, Q. Zheng, and G. S. Hayward. 2004. Early activation of the Kaposi's sarcoma-associated herpesvirus RTA, RAP, and MTA promoters by the tetradecanoyl phorbol acetate-induced AP1 pathway. J. Virol. 78:4248–4267.

76. Wang, X. T., P. Y. Liu, and J. B. Tang. 2006. PDGF gene therapy enhances expression of VEGF and bFGF genes and activates the NF-κB gene in signal pathways in ischemic flaps. Plast. Reconstr. Surg. 117:129–137.

77. Xie, J., H. Pan, S. Yoo, and S. J. Gao. 2005. Kaposi's sarcoma-associated herpesvirus induction of AP-1 and interleukin 6 during primary infection mediated by multiple mitogen-activated protein kinase pathways. J. Virol. 79:15027–15037.

78. Zhong, W., H. Wang, B. Herndier, and D. Ganem. 1996. Restricted expression of Kaposi sarcoma-associated herpesvirus (human herpesvirus 8) genes in Kaposi sarcoma. Proc. Natl. Acad. Sci. USA 93:6641–6646.